

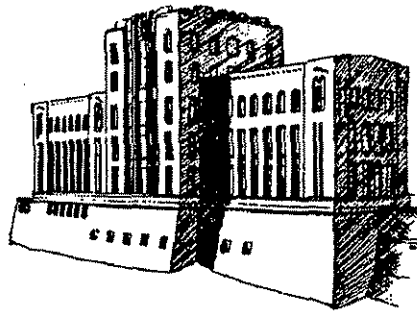
MEASUREMENT OF ICE SCRAPING FORCES ON SNOW-PLOW UNDERBODY BLADES

Iowa Department of Transportation Project HR 372

Final Report

by

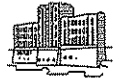
Wilfrid A. Nixon and James D. Potter



IIHR Technical Report No. 385

Iowa Institute of Hydraulic Research
College of Engineering
The University of Iowa
Iowa City IA 52242

February 1997



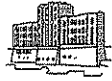
ACKNOWLEDGEMENTS

This project was made possible by funding from the Iowa Department of Transportation, Project Number HR 372. This support is gratefully acknowledged.

The support of the Director of the Iowa Institute of Hydraulic Research, Dr. V.C. Patel, enabled this study to proceed. The shop staff at IIHR, led by Mr. Jim Goss, made these experiments possible with their assistance. Experiments were assisted by Dr. Yinchang Wei. A special thanks goes out to Mr. Doug Houser and Mr. Mark Wilson.

The truck used in this testing was provided by the Iowa Department of Transportation. The trucks used in the full scale tests were provided by the Iowa Department of Transportation Oakdale shop. The assistance of Mr. Lee Smithson and Mr. Ron Stutzel throughout the project was appreciated. Permission to use the test site at the Coralville Reservoir was given by the US Army Corps of Engineers. A special thanks goes out to the Oakdale shop crew for all the extra maintenance work done on all the trucks that were involved in this project.

The opinions, findings, and conclusions expressed in this publication are those of the authors and not necessarily those of the Engineering Division of the Iowa Department of Transportation.



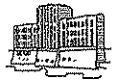
ABSTRACT

Ice or compacted snow on the roadway represents a severe winter hazard that can occur quite often in the winter months. There are three methods that are typically used to remove ice or compacted snow from the roadway: Chemical, mechanical and non-contact methods. The procedure commonly used consists of salting and sanding the roadway while using a front mounted plow and/or an underbody plow to remove snow and ice. This project builds upon project HR 334, with two major developments. In this study, several new cutting edges were tested in a series of closed road tests. These new cutting edges consisted of a variety of serrated shapes. The study also included measurement of ice scraping forces by in-service trucks. These in-service trucks were two Iowa Department of Transportation trucks from the Oakdale shop. These trucks were instrumented in a similar manner as the truck used in the closed-road tests. These trucks provided data from real life ice or compacted snow removal situations.

Results from the closed-road and in-service tests were analyzed by two parameters. The first parameter is the scraping effectiveness, which is defined as the average horizontal force experienced by a cutting edge. The amount of ice scraped from the roadway is directly proportional to the magnitude of the scraping effectiveness. Thus an increase in scraping effectiveness indicates an increase in the amount of ice being scraped from the roadway. The second parameter is force angle, which is defined as:

$$\text{Force Angle} = \text{Tan}^{-1} [\text{Vertical Force} / \text{Horizontal Force}]$$

A combination of a minimal force angle and a maximized scraping effectiveness represents a case in which the maximal amount of ice is being removed from the pavement without an exceptionally large vertical force. Results indicate that each cutting edge produced a maximal scraping effectiveness with a testing configuration of:



- Blade Angle = 15°
- Download Force = High (23,000 lbs)

Results also indicate that each cutting edge produced a minimal force angle with a testing configuration of:

- Blade Angle = 15°
- Download Force = Low (10,000 lbs)

Results from the in-service trucks produced similar data and also similar trends within the data when compared to the results of the closed-road tests. This result is most important, as it suggests that the closed-road tests do provide an accurate measure of ice scraping forces for a given blade and configuration of that blade. Thus if the closed-road tests indicate that certain blades perform well, there is now excellent reason to conduct full scale tests of such blades.



TABLE OF CONTENTS

ACKNOWLEDGMENTS	i
ABSTRACT.....	ii
LIST OF TABLES.....	vi
LIST OF FIGURES	vii
I. INTRODUCTION	1
II. EXPERIMENT DESCRIPTION	2
A. Underbody Plow	2
1. Range of Motion	2
2. Cutting Edges.....	5
3. Instrumentation	8
B. Calibration of Sensors.....	10
C. Pre-testing Procedure	10
D. Testing Procedure	10
E. Testing Matrix.....	11
III. RESULTS AND DISCUSSION	12
A. Conversion of Data	12
B. Definition of Effectiveness and Force Angle.....	15
C. Force Angle Results.....	15
1. Air temperature effects on force angle.....	19
2. Wear effects on force angle.....	20
D. Scraping Effectiveness Results	22
1. Air temperature effects on effectiveness.....	26
2. Wear effects on effectiveness.....	26
E. Modified Scraping Effectiveness Results	29
F. Visual Results	31
IV. DESCRIPTION OF ICE SCRAPING	37
A. Introduction.....	37
B. Standard Blade	37
C. Serrated Blade.....	39



V.	DESCRIPTION OF IN-SERVICE TRUCKS	40
A.	Truck Description	40
B.	Instrumentation	40
VI.	RESULTS AND DISCUSSION OF IN-SERVICE TRUCKS	41
A.	Description of Data Collection	41
B.	Comparison of Results	42
VII.	CONCLUSION	44
A.	Summary	44
B.	Future Research	46
C.	Implementation	47
	REFERENCES	49
	APPENDIX A	50
	APPENDIX B	60
	APPENDIX C	67



LIST OF TABLES

Table 1. Results of In-Service Tests41



LIST OF FIGURES

Figure 1.	IDOT truck used in conducting the tests.....	2
Figure 2.	Side view of underbody plow	3
Figure 3.	Definition of blade angle	4
Figure 4.	Definition of attack angle.....	4
Figure 5.	Configuration of blade one	5
Figure 6.	Geometry of blade two and three.....	6
Figure 7.	Geometry of blade four	7
Figure 8.	Picture of blade four on the underbody.....	7
Figure 9.	Computer system in support frame	9
Figure 10.	Digital displays that provide feedback of testing parameters	9
Figure 11.	Testing matrix	12
Figure 12.	Data from channels one, two and three during test seven.....	13
Figure 13.	Data from channel four during test seven	13
Figure 14.	Vertical and horizontal forces experienced by the cutting edge during test seven	14
Figure 15.	Blade angle during test seven	14
Figure 16.	Force angle for all test configurations based on blade angle	17
Figure 17.	Force angle for all test configurations based on increasing order.....	18
Figure 18.	Wear effects on a blade at 30°	19
Figure 19.	Air temperature effects on force angle for blade two	20
Figure 20.	Effects of wear on the force angle for blade two	21
Figure 21.	Maintaining a sharp cutting edge by changing the blade angle after it has become worn	22
Figure 22.	Scraping effectiveness for all blade configurations based on blade angle.....	23
Figure 23.	Scraping effectiveness for all test configurations based on decreasing order	24
Figure 24.	Average results for all testing configurations	25



Figure 25.	Air temperature effects on scraping effectiveness for blade one tests	26
Figure 26.	Effects of blade wear on scraping effectiveness for blade one tests ...	27
Figure 27.	Effects of blade wear on scraping effectiveness for blade two tests ...	27
Figure 28.	Effects of blade wear on scraping effectiveness for blade three tests ..	28
Figure 29.	Effects of blade wear on scraping effectiveness for blade four tests ..	28
Figure 30.	Modified scraping effectiveness for all blade configurations based on blade angle	30
Figure 31.	Modified scraping effectiveness for all test configurations based on decreasing order	31
Figure 32.	Typical ice sheet prior to testing	32
Figure 33.	Ice sheet after testing with blade one	32
Figure 34.	Ice sheet after testing with blade one	33
Figure 35.	Ice sheet after testing with blade two	33
Figure 36.	Ice sheet after testing with blade two	34
Figure 37.	Ice sheet after testing with blade three	34
Figure 38.	Ice sheet after testing with blade three	35
Figure 39.	Ice sheet after testing with blade four	35
Figure 40.	Ice sheet after testing with blade four	36
Figure 41.	Two zones of ice failure produced by an underbody plow	37
Figure 42.	Close up of ice being ejected from zone one	38
Figure 43.	Close up of ice being ejected from zone two	39
Figure 44.	Front view of serrated blade showing zones two and three of fracture	40
Figure 45.	Results of blade angle effects	42
Figure 46.	Download effects on force angle	43
Figure 47.	Download effects on horizontal force	44
Figure 48.	Descriptive placement of Pin A and Pin B relative to the horizontal and vertical force	62
Figure 49.	Descriptive placement of α , β and $F(1)$	62



Figure 50.	Plot of "X" and "Z" values for a six inch blade	63
Figure 51.	Angles required to determine moment produced by F(1)	64
Figure 52.	Angle β versus blade angle	65
Figure 53.	Plot of "X" and "Z" values for an eight inch blade	66



I. INTRODUCTION

Although driving in conditions hindered by snow and ice is normal for people living in the Northern Tier States of the U. S., road crews are still expected to remove snow quickly after a snow storm. Road crews typically use road salt and mechanical methods to remove snow and ice. Salt is required because mechanical methods are inefficient. Since the 1950's, salt has been used as an acceptable chemical for melting snow and ice from the roadway. However, by the mid 1970's, some negative side effects of salt began to be noted. It became apparent that water supply quality could be impaired by excessive salting of roads. Bridges and roadways may also suffer corrosion damage if salt is used excessively, as may road vehicles. Alternative chemicals have been considered and used to a limited extent, but, due to cost, road salt remains the most popular chemical used for winter maintenance. An improvement in the mechanical methods for snow and ice removal, so that these methods become more effective at removing ice and compacted snow, would reduce the amount of road salt applied to roads.

This project had two purposes. The first was to examine, using an instrumented truck in closed-road conditions, the effectiveness of different cutting edges for scraping ice. The cutting edges tested were serrated cutting edges, all mounted on an underbody plow. The results from serrated cutting edges were compared with those obtained for a regular cutting edge (tested previously, Nixon and Frisbie, 1993). The blades were tested at angles of 15° and 30° and at low and high download conditions. The second purpose was to measure the forces experienced by underbody plows in service conditions. To this end, two Iowa Department of Transportation (DOT) trucks were instrumented and scraping forces measured during the winter of 1995-96 (see Chapter VI). The forces thus measured are compared with the closed-road tests conducted both in this and a previous study. The aim of this part of the study was to ensure that results from the closed-road tests did carry over into true field situations.



II. EXPERIMENTAL DESCRIPTION

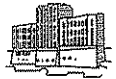
A. Underbody Plow. Tests were performed on a 1983 International Fleetstar S-1900 25 ton gross vehicle weight (GVW) dump truck on loan from the Iowa Department of Transportation (IDOT). The truck was fitted with an underbody plow which is located between the front and rear axles (see Figure 1). The underbody plow can be controlled by four levers, which are located in the cab of the truck. The levers control the two main cylinders, which provide the right and left download force, the blade angle and the blade attack angle. The benefit of using an underbody plow is the large download force it can apply to the ice. This download force results when a portion of the truck's weight is



Figure 1 IDOT truck used in conducting the tests

transferred from the tires to the blade. Thus, the maximum download force is directly related to the weight of the truck.

1. Range of Motion. The vertical range of the underbody blade is seven inches. Figure 2 shows the right side of the underbody plow. The cylinders responsible for rotating the cutting edge will be referred to as the 3rd cylinders. The two main



hydraulic cylinders shown in Figure 2 are responsible for the vertical download. The main hydraulic cylinders move the snow blade vertically by means of the triangular shaped links that rotate about the two rotation points. The 3rd cylinders are responsible for rotating the snow blade. The 3rd cylinders allow the cutting edge to rotate through a 70° range of motion. The blade angle is defined as the angle the cutting edge makes with the normal from the road surface, as shown in Figure 3. There are two 3rd cylinders rotating the snow blade; they act in parallel which allows the truck operator to maneuver both by using only one lever in the cab.

Due to irregularities that may exist on the roadway, the truck was equipped with a shock accumulator. When the truck encounters an irregularity on the roadway the cutting

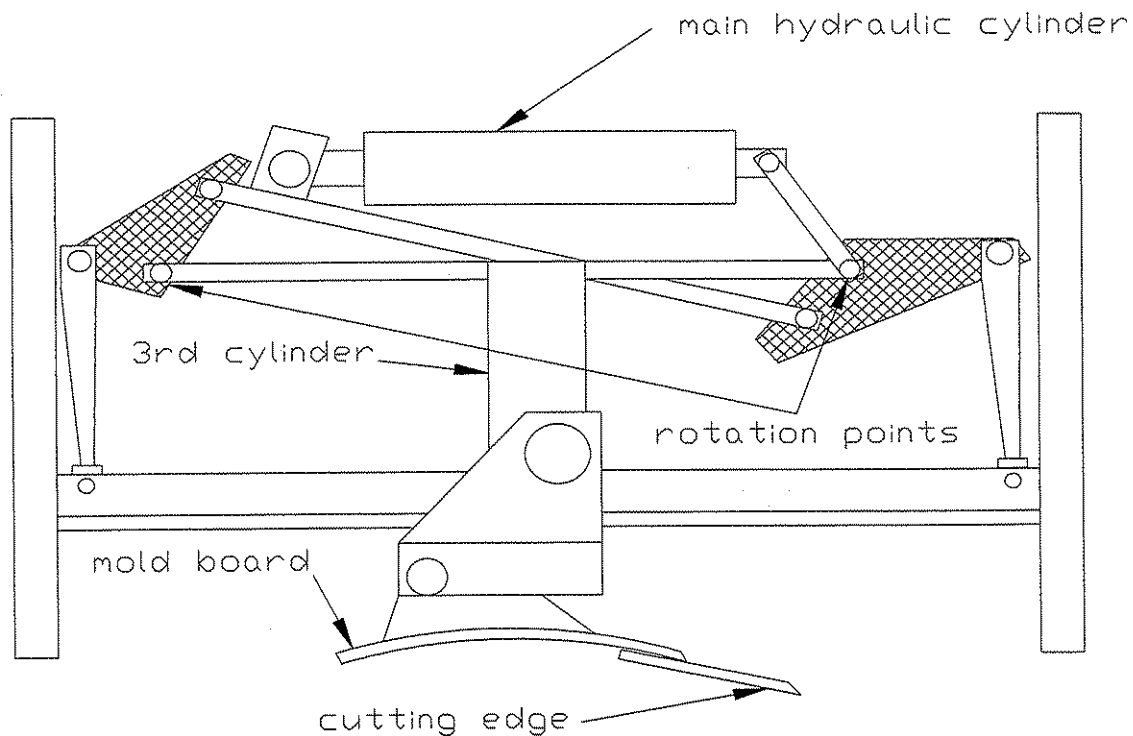


Figure 2 Side view of underbody plow

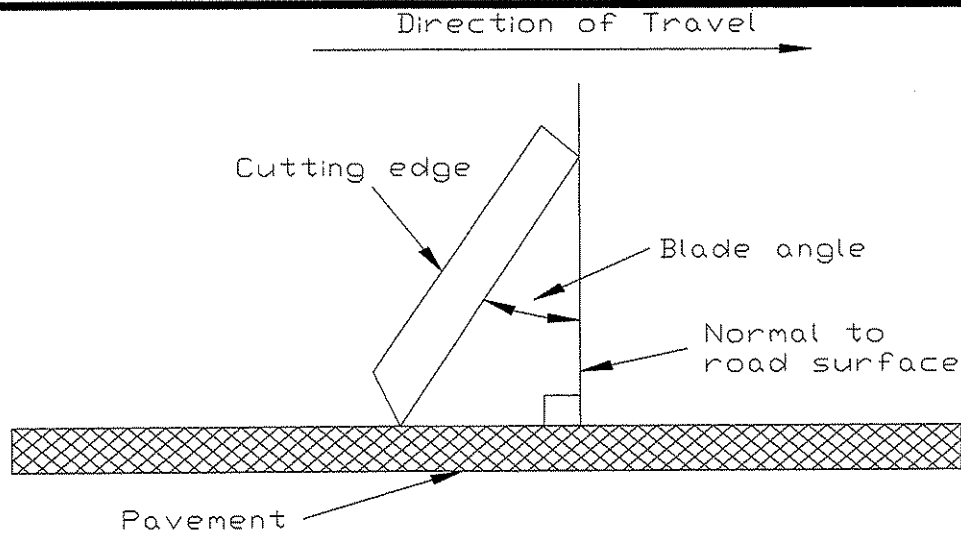


Figure 3 Definition of blade angle

edge will rotate back. This rotation diminishes any damage that might occur to either the roadway or the underbody. The hydraulic fluid that is forced out of the cylinder is collected in the shock accumulator. The truck operator may also adjust the attack angle of the snow blade. The attack angle is defined as the angle the cutting edge makes with the perpendicular to the direction of travel as shown in Figure 4. Adjusting the attack angle lets the truck operator direct the scraped ice and snow to either the left or right side of the truck.

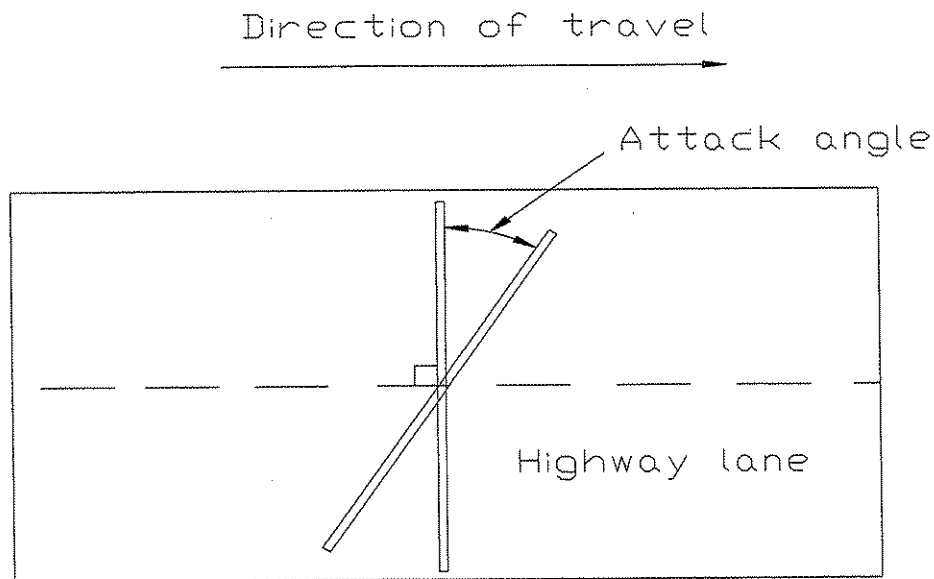


Figure 4 Definition of attack angle



2. Cutting Edges. The cutting edge or snow blade was bolted to the mold board. The mold board is shown in Figure 2. The research conducted was carried out using four different cutting edges. The first was a carbide insert cutting edge manufactured by Pacal Blades. This cutting edge consisted of two sections with each section being $3/4 \times 6 \times 48$ inches ($1.9 \times 15.2 \times 121.9$ cm). The geometry of this cutting edge is shown in Figure 5. This type of cutting edge was also tested in project HR 334. This cutting edge was used to provide a control between the tests conducted in the present research and those conducted in HR 334. However, there were some differences between the two

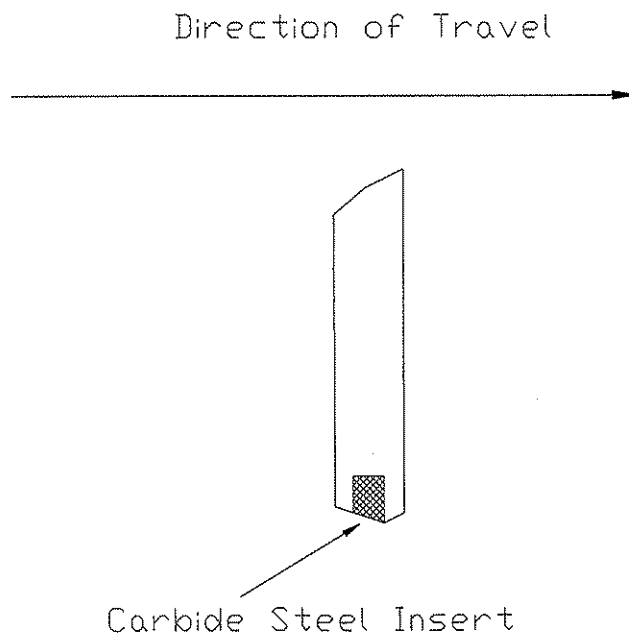
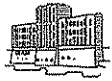


Figure 5 Configuration of blade one

underbody plows used in this project and in HR 334. These differences include different ranges of vertical movement of the cutting edge and different ranges of blade angle. However, after careful review, it was determined that the changes between the two plows were sufficiently minor that direct comparison between the two series of tests would be appropriate.

The final three cutting edge designs were based on serrated shapes, and were also manufactured by Pacal Blades. Like the first cutting edge, each of these cutting edges



consisted of two sections, but each section was $3/4 \times 8 \times 48$ inches ($1.9 \times 20.2 \times 121.9$ cm). Cutting edge two and three consisted of shapes with a tooth to gap ratio of 1.5/1.0. Cutting edge two was based on an elliptical pattern while cutting edge three was based on a triangular pattern. Cutting edge four consisted of a dual blade configuration that had a tooth to gap ratio of 1.0/1.5. This dual cutting edge configuration consisted of two cutting edges bolted back to back to the mold board. The two cutting edges are horizontally and vertically offset from each other. The purpose of the horizontal offset was to reduce the amount of unscraped ice. The horizontal offset aligned the teeth of one cutting edge with the gaps of the other cutting edge. A vertical offset was required to ensure both cutting edges were in contact with the ice during tests. The offset was accomplished by altering the vertical and horizontal position of the bolt holes on each of the cutting edges. The vertical offset was 0.3 inches (.75 cm) while the horizontal offset was 1.25 inches (3.2 cm). The geometries of cutting edge two and three are shown in Figure 6 while cutting edge four is shown in Figure 7. Figure 8 shows a picture of cutting edge four to help clarify its design.

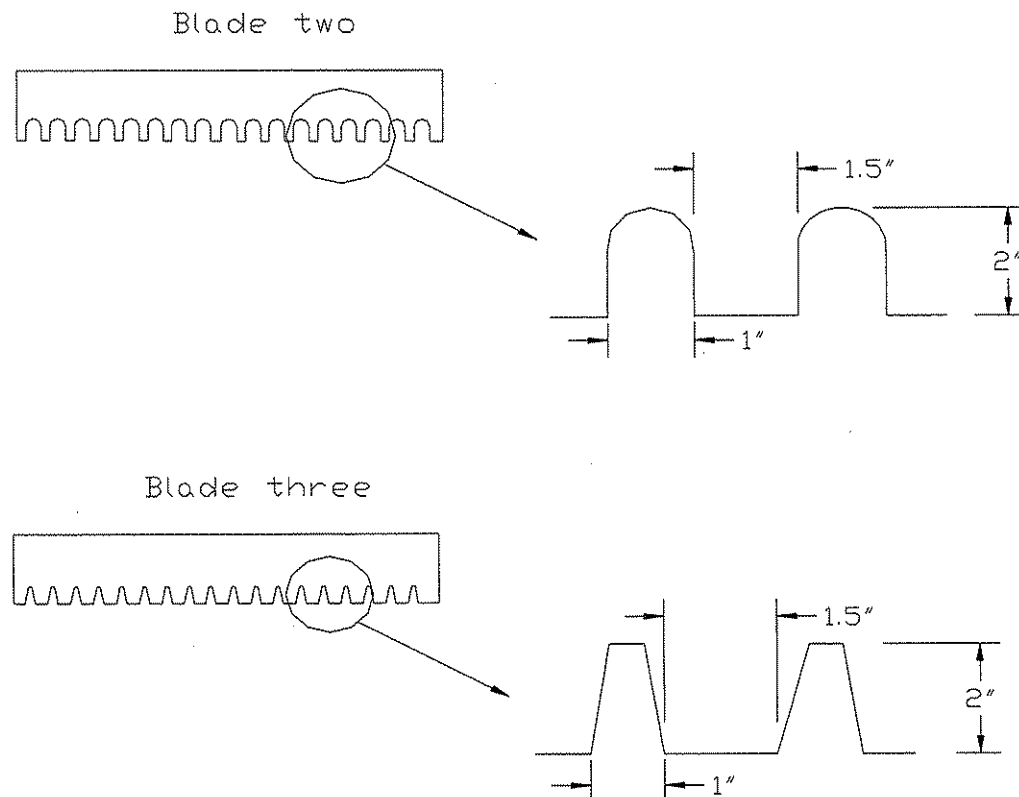


Figure 6 Geometry of blade two and three

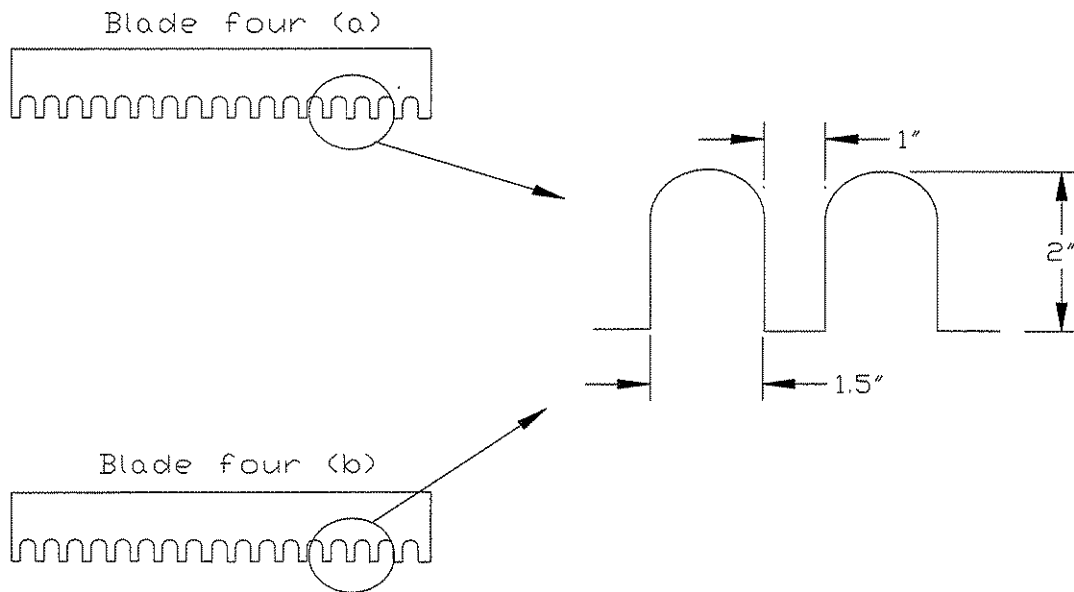


Figure 7 Geometry of blade four

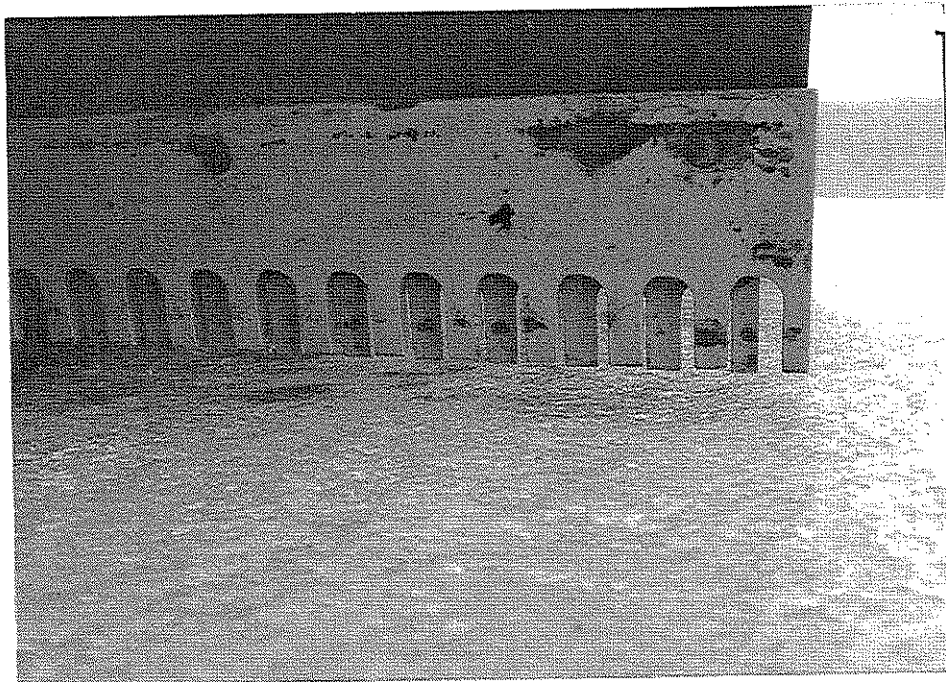


Figure 8 Picture of blade four on the underbody



3. Instrumentation. The underbody mechanism was fitted with three pressure sensors and an inclinometer. The three pressure sensors were manufactured by Lucas Control Systems Products, type number P 1241-0005. Two pressure sensors were used for the left and right main cylinders while one pressure sensor was used for the 3rd cylinder. The pressure sensor converts a given line pressure into a voltage signal which can be recorded by a computer. The range of these pressure sensors is 0 - 3500 psi (gauge) which would produce a voltage signal of 0 - 5 volts.

The blade angle was measured by using an inclinometer which was attached to the back of the mold board. The inclinometer was a Schaevitz Angle Star Protractor which would produce of voltage signal between 0 and 10 volts, depending on the angle orientation. For its protection the inclinometer was encased in metal piping and bolted to the mold board.

All voltage signals were recorded by a personal computer (PC) that was inside the cab of the truck. The PC was manufactured by CyberResearch Incorporated and had an Intel 80486 processor. This PC was chosen because it was built with the monitor, keyboard and processor all within a sturdy case as shown in Figure 9. This particular design allowed normal data acquisition even though the testing environment was very unsteady with significant vibration. An analog to digital card was placed in the computer to record the voltage signals during the tests. A DAS-1600 Series Function Call Driver was installed in the PC for this purpose. The PC's hard drive recorded the signals while a code written in basic analyzed the data. The code provided visual results of the data immediately after completing a test.

The power for the computer and the sensors was provided by two car batteries located inside the cab. These batteries were required because power provided by the truck batteries produced undesired noise in the data. To allow the driver instantaneous feedback during the testing, four digital displays were installed in the computer frame. Figure 9 shows the computer setup while Figure 10 shows a close up of the digital displays. The values that were displayed were the current blade angle, the two download forces and the pressure in the 3rd cylinders.

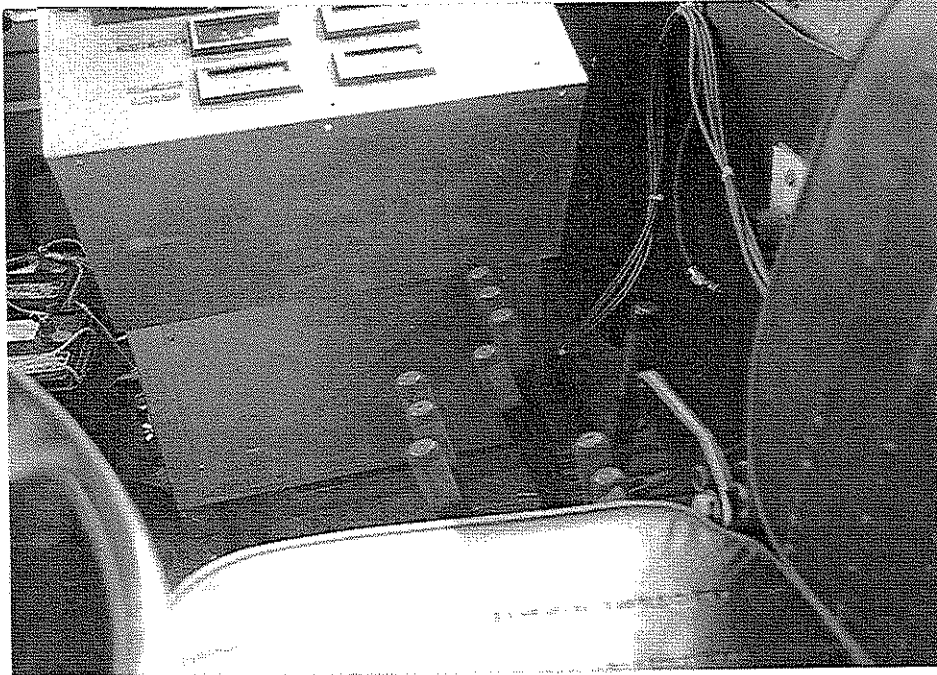


Figure 9 Computer system in support frame



Figure 10 Digital displays that provide feedback of testing parameters



B. Calibration of Sensors. Relating a force to a voltage signal was accomplished by calibrating the pressure sensors. The two main cylinders were calibrated by applying a range of known vertical forces to the snow blade and recording the voltage signal. The vertical load was produced by using a 10 ton jack attached to a pressure gauge. The pressure gauge was used to determine the applied vertical force to the snow blade. Changing the magnitude of the vertical force and recording the voltage signal resulted in data that produced a linear relationship.

The blade angle was calibrated in a similar manner. The blade angle was related to a voltage signal by recording the voltage signal and measuring the blade angle with an electronic protractor. A relationship between voltage signal and blade angle was determined by plotting blade angle versus voltage signal. This relationship was also linear.

C. Pre-testing Procedure. All tests were conducted at the Coralville Reservoir Spillway located five miles north of Iowa City. This site was chosen because the large spillway apron was relatively flat and closed to the public in the winter months. The tests were conducted on multiple slabs of concrete with each slab of concrete being 25 x 180 feet in size with expansion joints located every 30 feet along the 180 foot dimension.

The ice sheet was formed using a 750 gallon water tank located on another IDOT truck. The desired ice thickness was between 1/4" to 1/2" (0.64 cm to 1.3 cm). This thickness was accomplished by driving the IDOT truck back and forth over the same path while spraying a fine mist of water that covered a 25 foot wide path. It required 40 minutes to empty the water tank and produce the desired ice sheet. The ice sheet was ready for testing immediately or within six to seven hours depending on the air temperature.

D. Testing Procedure. All tests were conducted using the IDOT truck which was weighted down with one inch rock to provide more traction on the ice. The total weight of the truck with the rock was 48,000 lbs.



Prior to each test the air temperature and ice thickness were recorded on the computer. Also prior to each test the blade angle was set to the desired value. Each test started approximately 150 feet before the ice sheet. This allowed ample time for acceleration to reach the desired speed. After the truck reached approximately 10 mph, the download force was gradually applied until the desired download was achieved. As soon as this pressure was obtained, a button that activates the data-acquisition system was pushed. The data acquisition stopped after fifteen seconds of testing had occurred, or when the driver pushed any key on the keyboard.

After each test the general condition of the ice sheet was examined. The amount of ice removed and any patterns left on the ice by the given snow blade were noted. The information helped correlate a relationship between the amount of ice removed and the horizontal force. Pictures were taken of the ice sheet before and after a test to provide visual results.

E. Testing Matrix. The parameters studied in the tests were download force, blade angle and cutting edge configuration. Two ranges of download forces, low and high, were tested on each blade configuration previously discussed. The values of low and high download forces were 10,000 lbs and 23,000 lbs, respectively (Nixon and Frisbie 1993). The blade angle was tested at two different angles, 15° and 30°. The complete testing matrix (cutting edge, date of testing, low/high download force and blade angle) is shown in Figure 11. Cutting edge one was unable to reach a high download force because the cutting edge's height was only six inches while the other three cutting edges' height was eight inches. Since the underbody's vertical range of motion is limited to only seven inches, a blade would be unable to reach the high download force if its height was less than approximately seven inches.

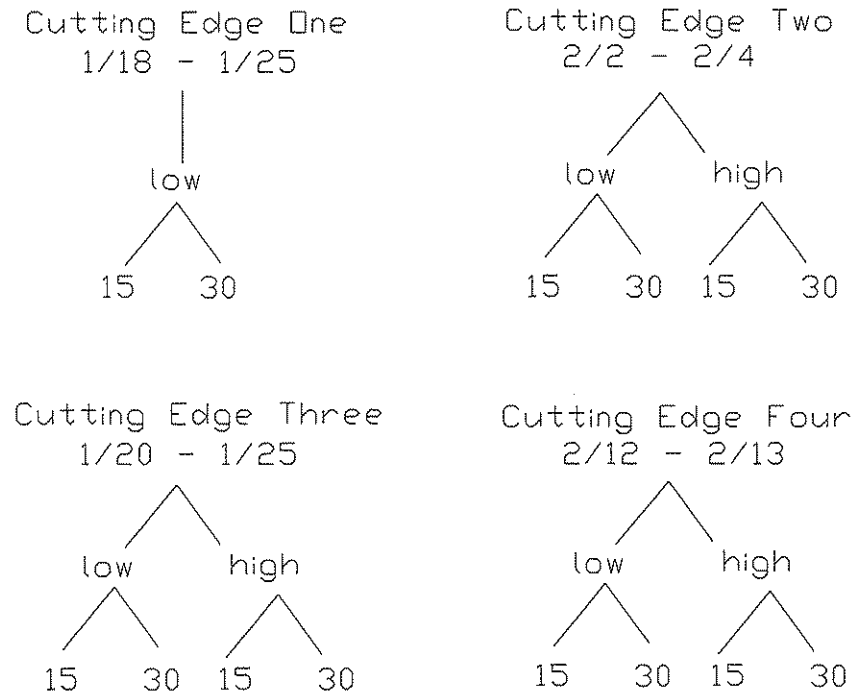


Figure 11 Testing matrix

III. RESULTS AND DISCUSSION

A. Conversion of Data. Figure 12 and Figure 13 display (as an example) the data collected for test seven. The parameters for test seven were: blade three, low download pressure and a 15° blade angle. Channel one and two represent the voltage signals for the two main cylinders, while channel three is the voltage signal for the 3rd cylinders. Lastly, channel four is the voltage signal for the blade angle.

Converting the voltage signals into the desired units was accomplished by using the calibration curves previously discussed. The two channels responsible for the vertical force were channel one and two. Thus, the vertical force was determined by summing channels one and two, then this total was converted into a force by using its calibration curve. The blade angle was determined by using the voltage signal from channel three and its corresponding calibration curve. To determine the horizontal force the following parameters were required: vertical force, blade angle and pressure in the 3rd cylinder.

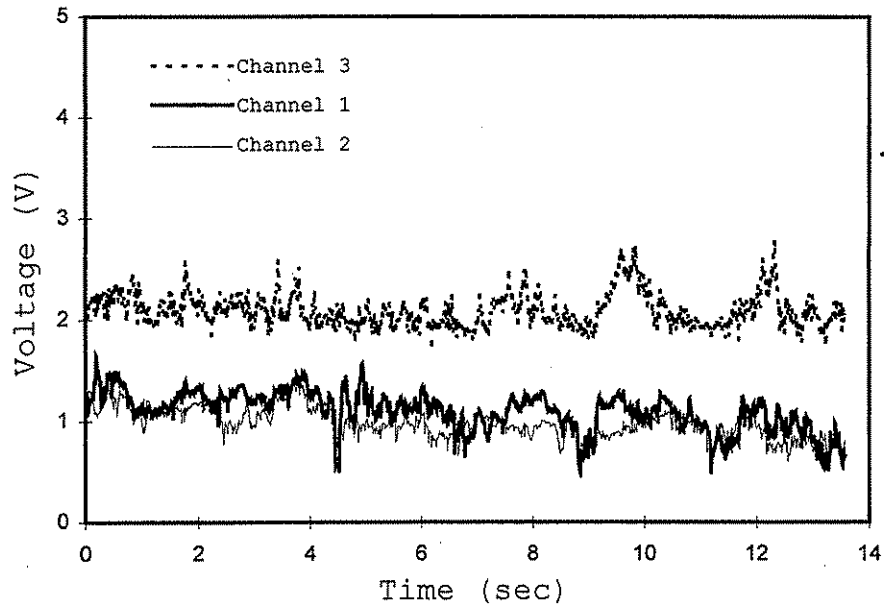


Figure 12 Data from channels one, two and three during test seven

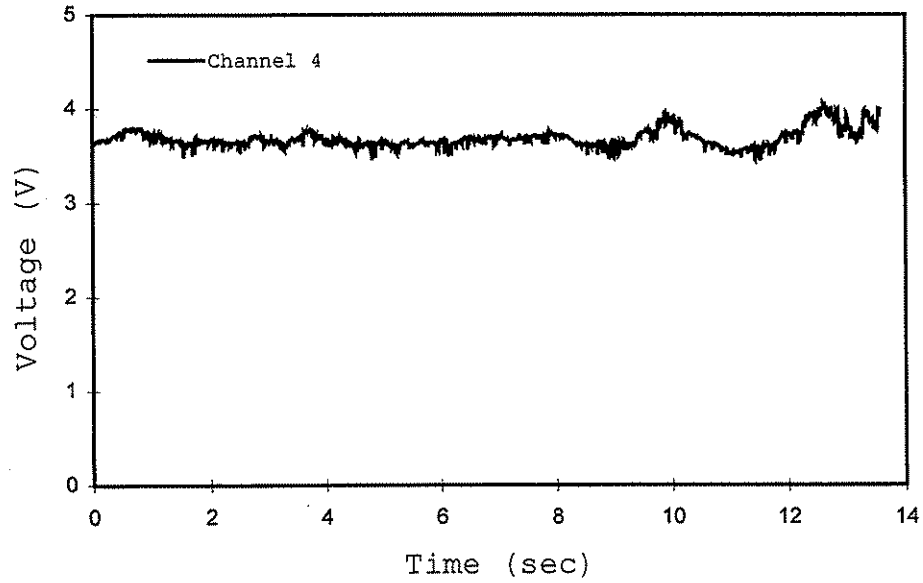


Figure 13 Data from channel four during test seven



The method for determining the horizontal force is presented in Appendix B.

Figure 14 represents the vertical and horizontal force versus time for test seven. Figure 15 displays the blade angle for test seven.

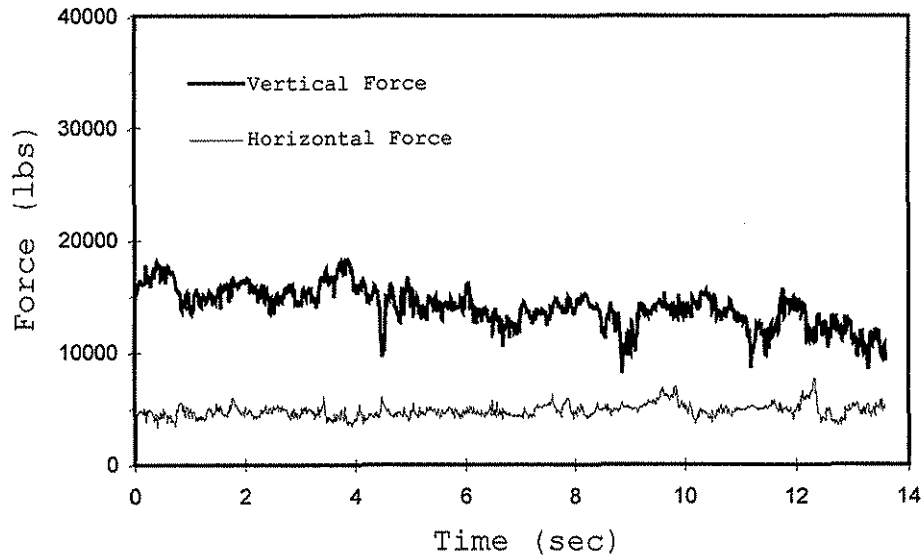


Figure 14 Vertical and horizontal forces experienced by the cutting edge during test seven

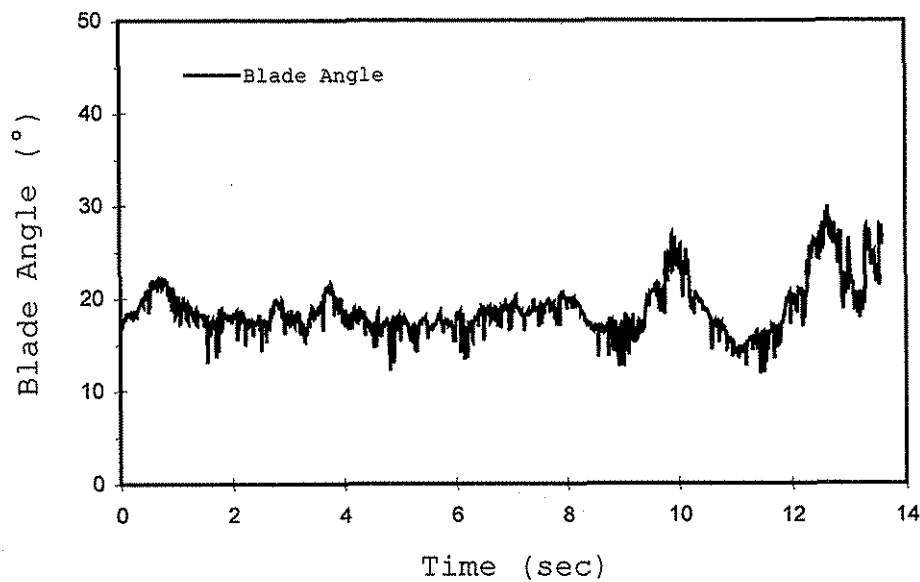


Figure 15 Blade angle during test seven



B. Definition of Effectiveness and Force Angle. One goal of the research was to determine the testing configuration for maximum ice removal. It was also important that the ice was scraped in a manner that allowed the truck operator to maintain complete control of the truck at all times. If a majority of the truck's weight rests on the cutting edge, the truck operator would have very little control of the truck.

Scraping effectiveness and force angle are defined as terms that evaluate each test's performance. The scraping effectiveness is defined as the effectiveness of the cutting edge in scraping ice from the pavement. As discussed in Nixon and Frisbie (1993), the amount of ice scraped is directly related to the magnitude of the horizontal force. Thus, the scraping effectiveness is equivalent to the horizontal force. The force angle is defined as:

$$\text{Force Angle} = \text{Tan}^{-1} [\text{Vertical Force} / \text{Horizontal Force}]$$

The optimum results of a test would be a large scraping effectiveness coupled with a minimal force angle. A large scraping effectiveness is required to ensure that the ice is being scraped from the pavement. A minimal force angle helps insure that a large scraping effectiveness is not being obtained by an excessively large vertical force. These two terms had to be evaluated side by side to ensure the optimum conditions were being obtained. The force angle does not relate directly to the amount of ice being removed by the cutting edge. For example, a force angle of 76° could result from a vertical force of 20,000 lbs and a horizontal force of 5,000 lbs. This ratio could also be obtained by a vertical force of 8,000 lbs and a horizontal force of 2,000 lbs. The first example would remove more ice from the pavement than the second case. However, the first case represents a situation where the truck operator may not have complete control of the truck. It was important to compare the force angle to the scraping effectiveness in order to evaluate the test results properly.

C. Force Angle Results. Evaluation of force angle allows a comparison to be made between the four blades. A minimal force angle is one of the desired conditions



when scraping ice occurs. The results for all test configurations are shown in Figure 16. The average for each testing configuration is graphed with its corresponding standard deviation (shown as a vertical bar – those points with no vertical bar had very small standard deviations). Each test was placed in either the 15° or 30° blade angle case, even though their mean values may have been slightly different. The standard deviation points out how excessive wear on a blade can effect the results. This is discussed in detail below. Figure 17 shows the force angle for all test configurations in ascending order of force angle. The test configurations in Figure 17 are described on the X-axis by blade number, blade angle and download pressure.

As shown in Figure 16, the force angle for blade one did not significantly change between blade angles. Since it was not possible to reach a high download pressure, only low download force data was plotted. The average value at the 15° blade angle was similar to the value obtained in past research (Nixon and Frisbie 1993). The average value at the 30° blade angle for this project was smaller than the value obtained in past research; current results had an average value of about 68° while the past research had an average value of 76°. However, the difference between test series is not statistically significant. The importance of testing blade one was to ensure that the results of this project were similar to the results in the previous research (Nixon and Frisbie 1993). Even though the new results were not exactly the same as the previous results, the similarities between the two are very encouraging.

The results obtained for blade two were expected. For both download pressures the 15° blade angle had force angle less than the corresponding 30° blade angle. This behavior was expected because of the method used to determine the horizontal force, refer to Appendix B. This method determined the horizontal force by summing moments about a pin, which was located on the underbody. The moment arm for the vertical force significantly increased from a 15° blade angle to a 30° blade angle. The other forces included in the equation had only minor changes in their moment arms. Thus, for a 30° blade angle the larger moment arm decreased the magnitude of the horizontal force. This decrease in magnitude was a result of an significant increase in the moment produced by the vertical

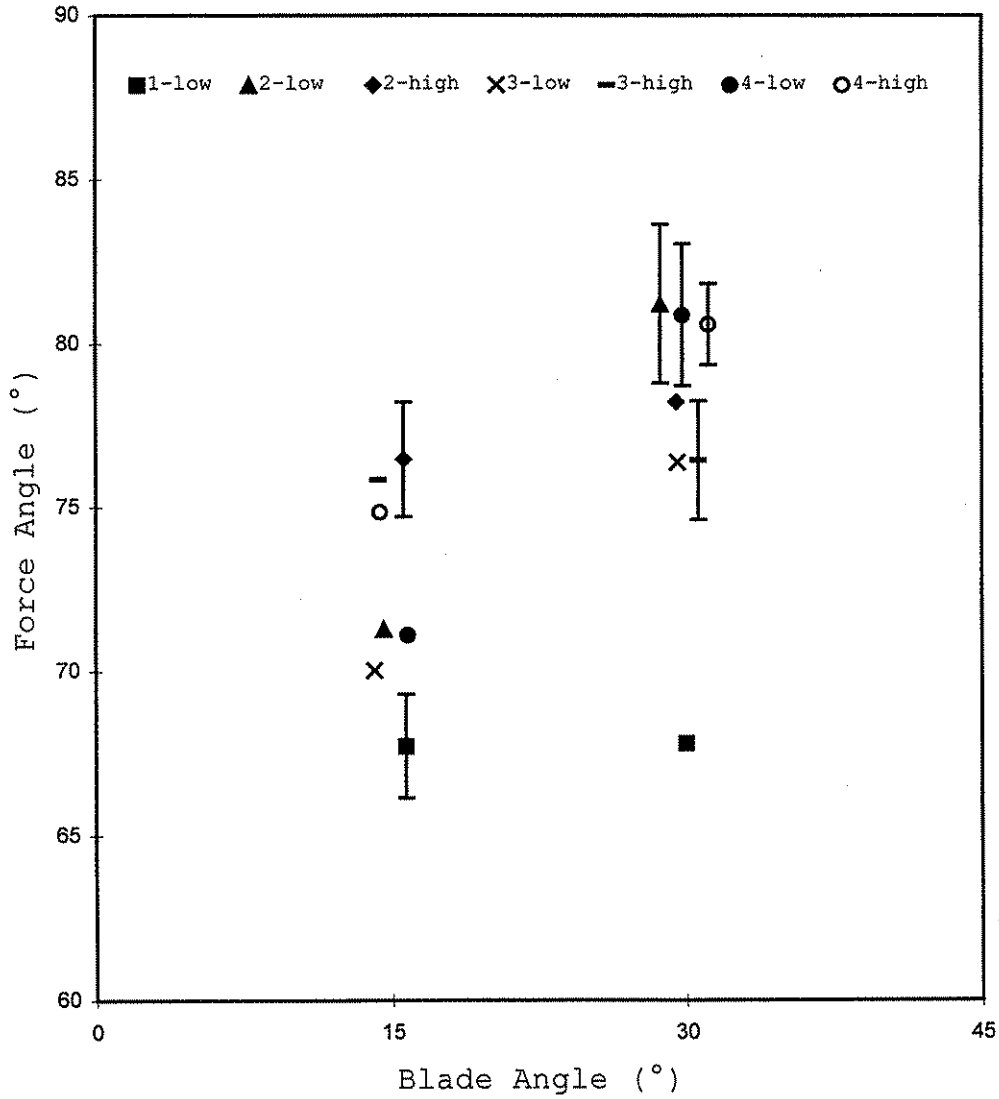


Figure 16 Force angle for all test configurations based on blade angle

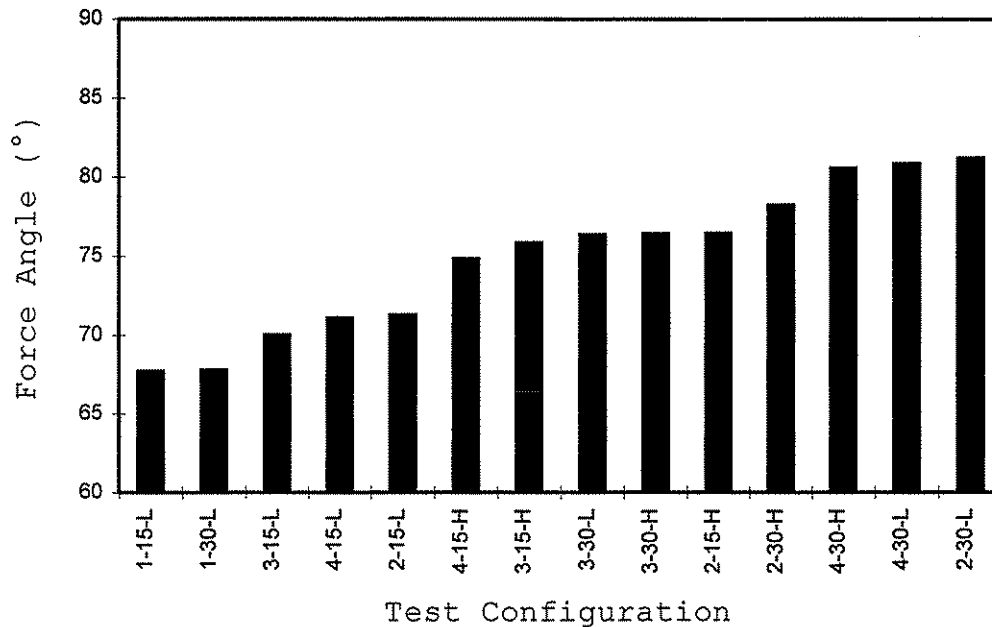


Figure 17 Force angle for all test configurations based on increasing order

force. If tests were able to be conducted at a blade angle of 0° , the force angle would be expected to be less than that obtained for a blade angle of 15° .

The standard deviation for the blade two data in Figure 16 shows a large variation in values for the low download pressure at a 30° blade angle. This may be explained by the difficulty a worn cutting edge has digging into the ice. The cutting edge was worn down quite quickly when compared to blade one. The excessive wear can be attributed to the serrated shape of the cutting edge. Blade two has only 58 inches of cutting edge in contact with the ice sheet, while blade one has 96 inches. The serrated shape of the cutting edge does increase the amount of stress the cutting edge can apply to the ice sheet. Larger stresses result in more ice being scraped from the roadway, but also increase the amount of wear on the blade. These large stresses eventually wear down the tip of the blade, resulting in an increase of cutting edge in contact with the ice. Figure 18 shows a cutting edge before and after excessive wear.

The average force angle for blade three, as shown in Figure 16, had patterns similar to blade two. The low download case showed an increase in force angle between the 15° and 30° blade angle cases. The high download case, in contrast, showed no



significant increase in force angle.

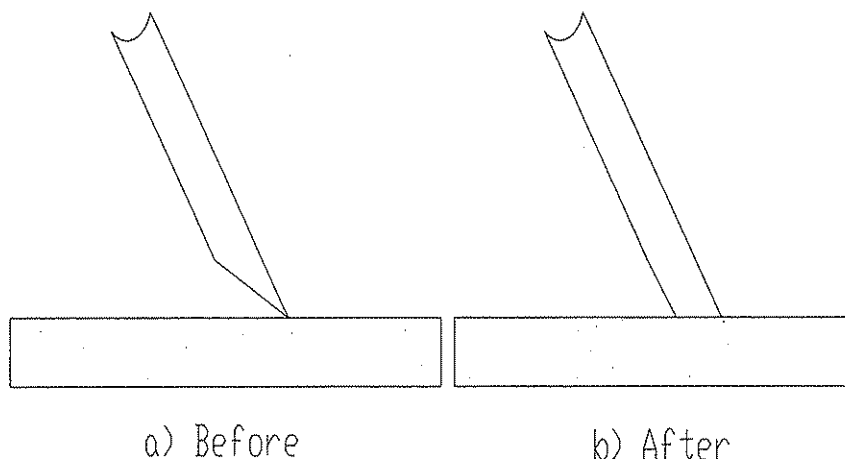


Figure 18 Wear effects on a blade at 30°

The results for force angle versus blade angle for blade four, shown in Figure 16, also followed previously discussed trends. Once again, a large standard deviation was shown for a 30° blade angle. This large scatter of data cannot be explained by wear effects (as was the case for blade 2). Blade four had 76 inches of cutting edge in contact with the ice sheet, which is 18 inches more than blades two and three. This increase prevented blade four from wearing down as quickly as blade two and three because of the decrease in stress at the tip of the cutting edge.

The force angles for all the test configurations are shown in Figure 17. Generally, lesser force angles resulted from tests conducted at 15° blade angles with a low download pressure. It can be seen from Figure 17 that increasing the download pressure by a factor did not result in an increase in the horizontal force by this same factor.

1. Air temperature effects on force angle. The air temperature was recorded prior to each test, using an electronic thermometer which recorded the temperature to the nearest 0.1°F (0.056°C). Plotting air temperature versus force angle shows the effects air temperature had on force angle. Conducting tests over a wide range of temperatures was not possible. Figure 19 shows a typical plot of force angle versus air temperature.

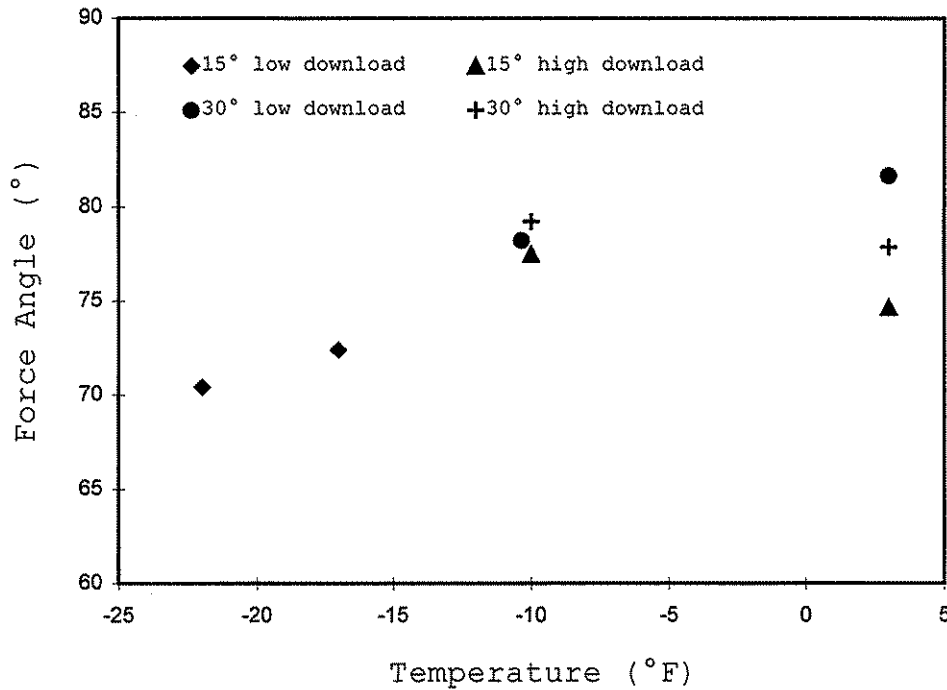


Figure 19 Air temperature effects on force angle for blade two

Even with the limited number of tests with varying air temperatures, there did not appear to be a relationship between air temperature and force angle. For example, Figure 19 shows two download cases that have an increase in force angle with an increase in temperature, while the remaining two download cases exhibit the opposite trend. It appears that air temperature has less effect on force angle than does download or blade angle.

2. Wear effects on force angle. A variable that could not be controlled, but is very important in scraping ice, was the sharpness of the cutting edge. A sharp cutting edge has a smaller amount of surface area in contact with the ice as compared to a dull cutting edge. A sharp blade will produce a larger stress field between the cutting edge and the ice as compared to the dull cutting edge. A larger stress field will result in more ice being removed from the pavement. Blade two was the only blade that showed significant wear. The plot of the force angle in chronological order for blade two is shown in Figure 20.

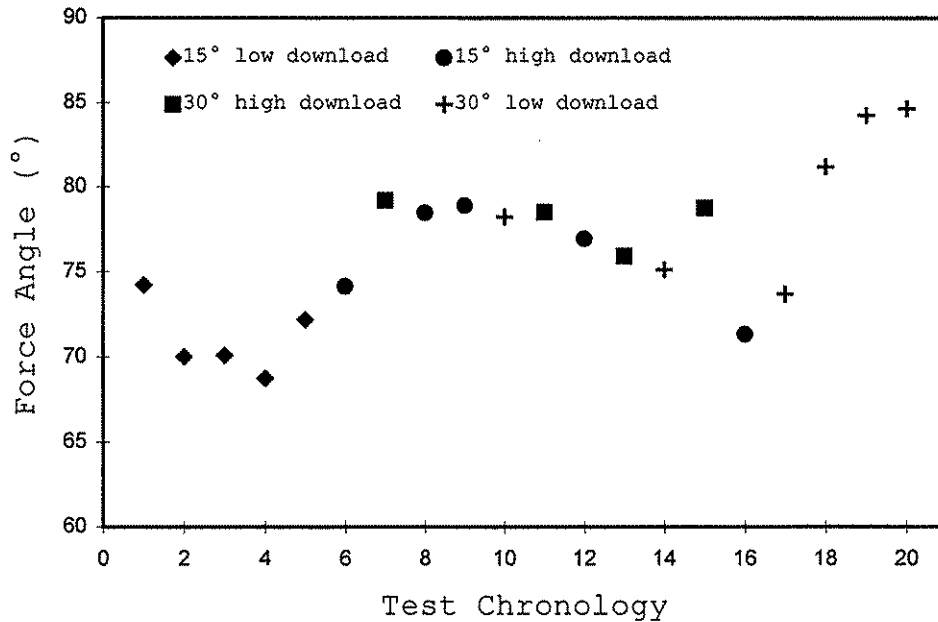


Figure 20 Effects of wear on the force angle for blade two

The last four tests in Figure 20 did show a significant increase in force angle. This increase in force angle is a result of a decrease in the horizontal force. As more and more tests are conducted at the same blade angle, the edge of the blade eventually becomes completely flat. A flat edge (see Figure 18) produces a reduced stress in the ice. The observed smaller horizontal force is a result of the cutting edge just grazing the top of the ice sheet and not actually digging into the ice. A sharper edge leads the cutting edge to dig into the ice sheet and produce a larger horizontal force.

Figure 20 also shows how the blade angle changed from test to test for tests six through sixteen. Changing the blade angle from test to test prevents the blade tip from becoming blunt, as seen in Figure 18. Figure 21 shows how changing the blade angle helps keep a relatively sharp point on the cutting edge.

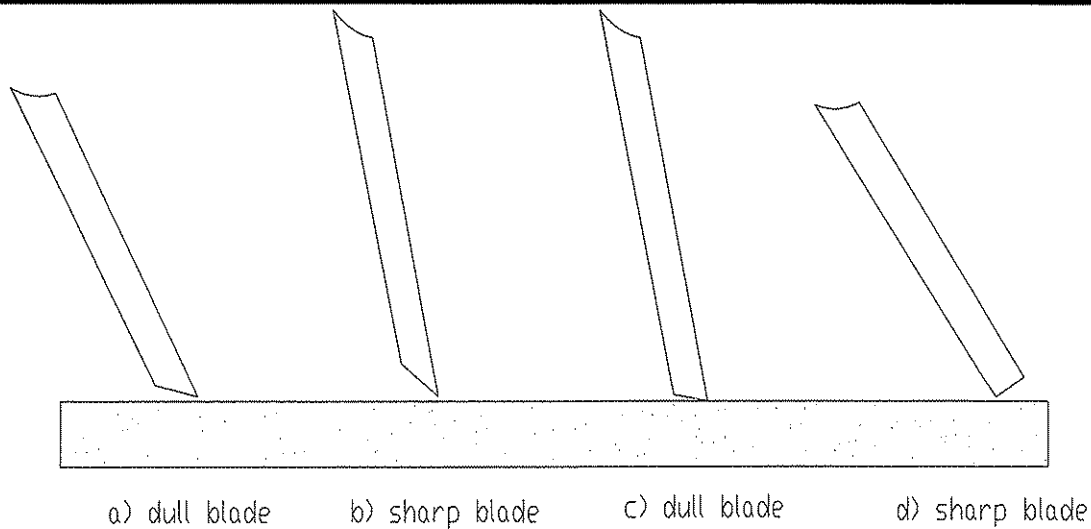


Figure 21 Maintaining a sharp cutting edge by changing the blade angle after it has become worn

D. Scraping Effectiveness Results. The scraping effectiveness of a cutting edge was defined as the average horizontal force experienced by the cutting edge during a test. The magnitude of the scraping effectiveness is directly related to the amount of ice scraped from the pavement, thus, the optimal results occur when the scraping effectiveness is maximized .

The results for all test configurations are shown in Figure 22. The average scraping effectiveness and corresponding standard deviation is graphed for each test configuration. Once again each test was placed in either the 15° or 30° blade angle category. Figure 23 shows the scraping effectiveness of all test configurations in descending order of effectiveness. The test configurations in Figure 23 are described on the X-axis by blade number, blade angle and download pressure.

It is expected that the scraping effectiveness would decrease with an increase in blade angle, assuming a constant download force. The results for blade 1 (see Figure 22) show a slight decrease in scraping effectiveness. This decrease in scraping is much less than that observed for the other three blades.

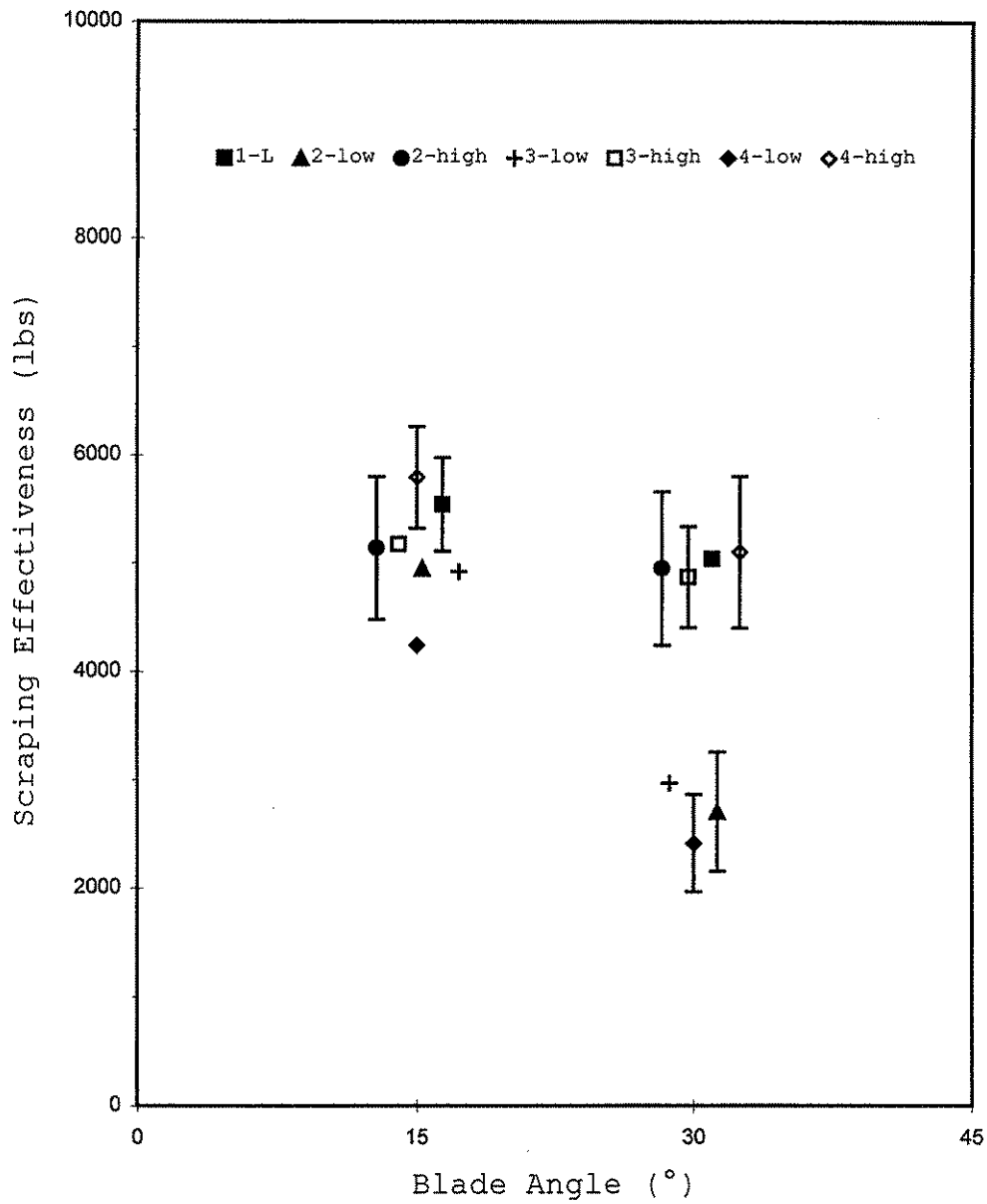


Figure 22 Scraping effectiveness for all blade configurations based on blade angle

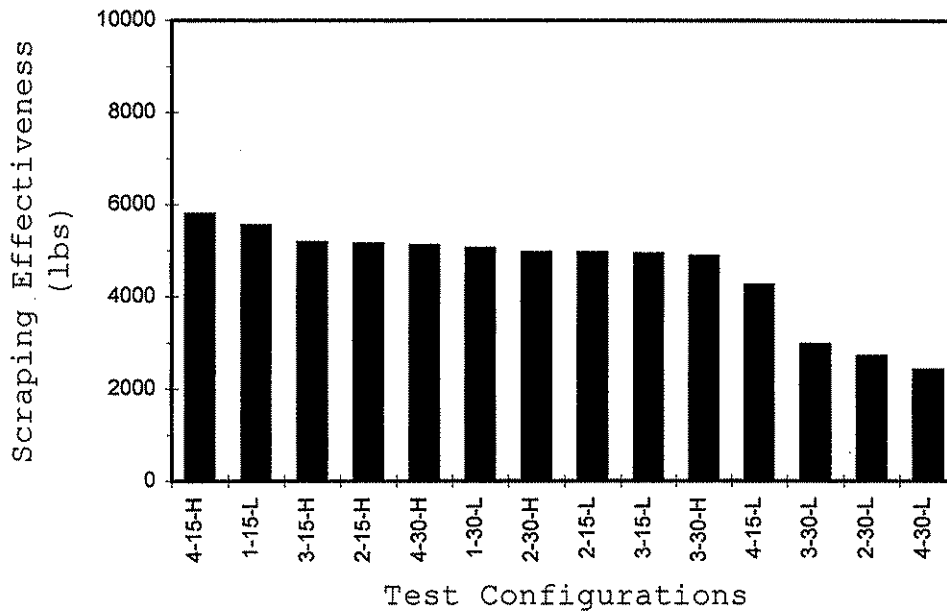


Figure 23 Scraping effectiveness for all test configurations based on decreasing order

Figure 22 also shows the results for blade two though blade four. All three blades show a decrease in scraping effectiveness when comparing the 15° low download results to the 30° low download results. The figure also show a slight decrease in scraping effectiveness when comparing the 15° high download results to the 30° high download results. The slight decrease in scraping effectiveness for both high download cases may be the result of the difficulty of obtaining the same high download force for each test. The high download forces ranged between 18,000 lbs and 27,000 lbs while the low download forces ranged between 9,000 lbs and 14,000 lbs. The difference among the high download forces may distort any correlation that may exist between the 15° and 30° high download cases. If this difference could be minimized then a correlation similar to the one for the low download tests would probably be found.

Figure 23 shows the scraping effectiveness results obtained for all testing configurations. Typically the larger scraping effectiveness values were obtained from high download tests. The vast majority of the test configurations had scraping effectiveness values between 5,000 and 5,800 lbs. The four tests that did not fall into this category were obtained by low downloads and three out of these four had values well



below the others. Figure 24 shows a plot of horizontal force versus vertical force for all test configurations.

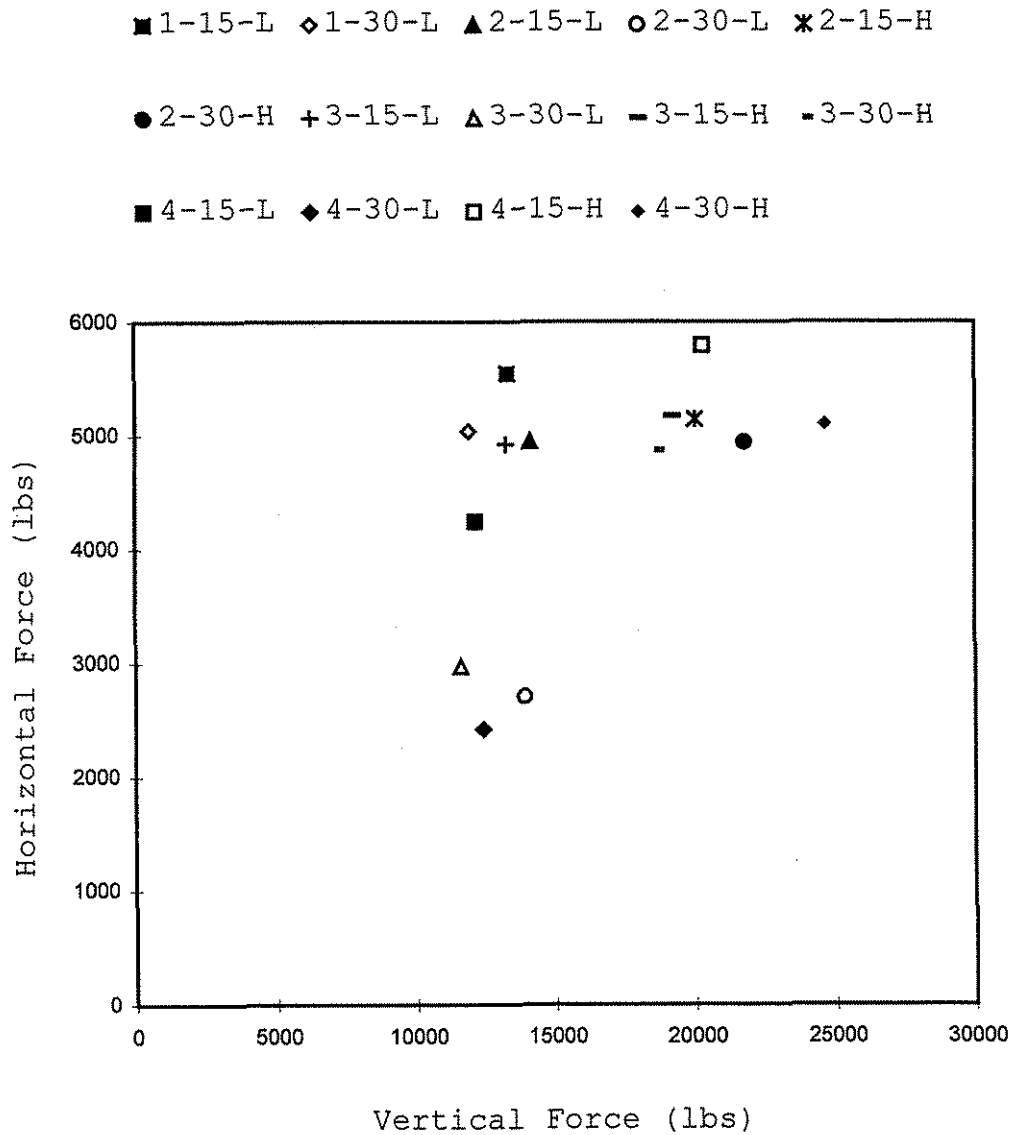


Figure 24 Average results for all testing configurations



1. Air temperature effects on effectiveness. To investigate the effects of air temperature on scraping effectiveness, these two parameters were plotted against each other. Figure 25 show the typical result of air temperature on the average scraping effectiveness for a given blade.

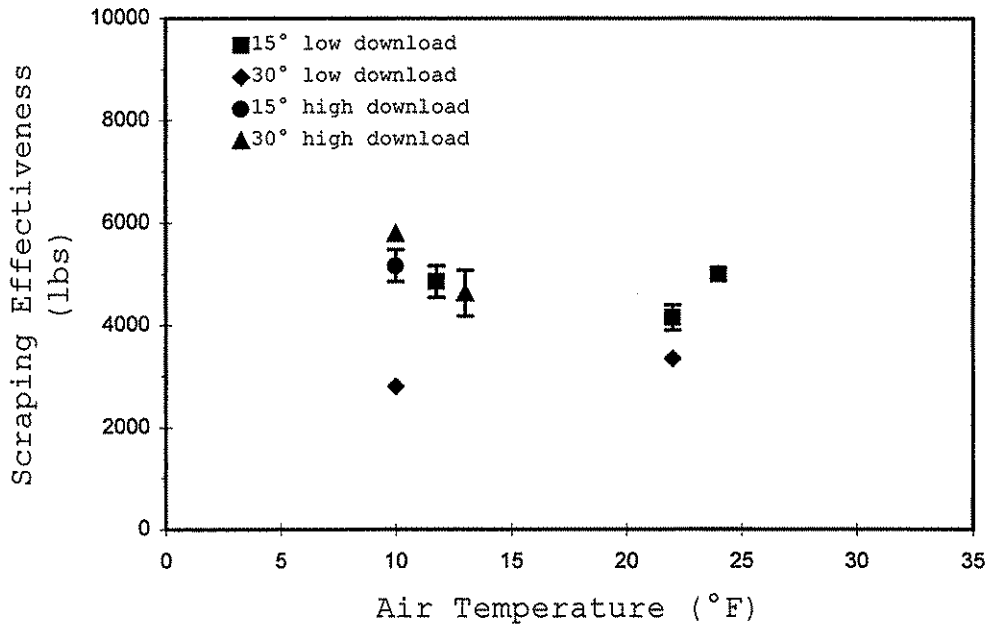


Figure 25 Air temperature effects on scraping effectiveness for blade three tests

Again, as for the force angle, there does not appear to be a correlation between scraping effectiveness and air temperature.

2. Wear effects on effectiveness. The scraping effectiveness was plotted versus the test chronology for each blade in Figure 26 through Figure 29. These figures attempt to show the effect of wear on the scraping effectiveness.

Two general statements can best summarize the results from Figure 26 through Figure 29. Firstly, Figure 27 shows some wear effects for the tests conducted at 30° blade angle with a low download pressure. The horizontal load for tests 17 through 20

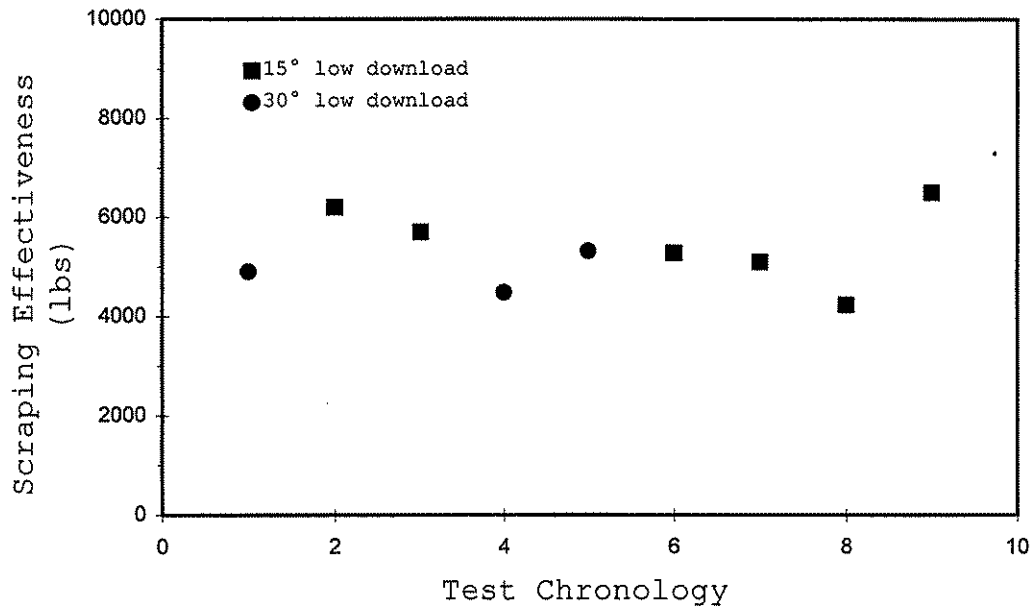


Figure 26 Effects of blade wear on scraping effectiveness for blade one tests

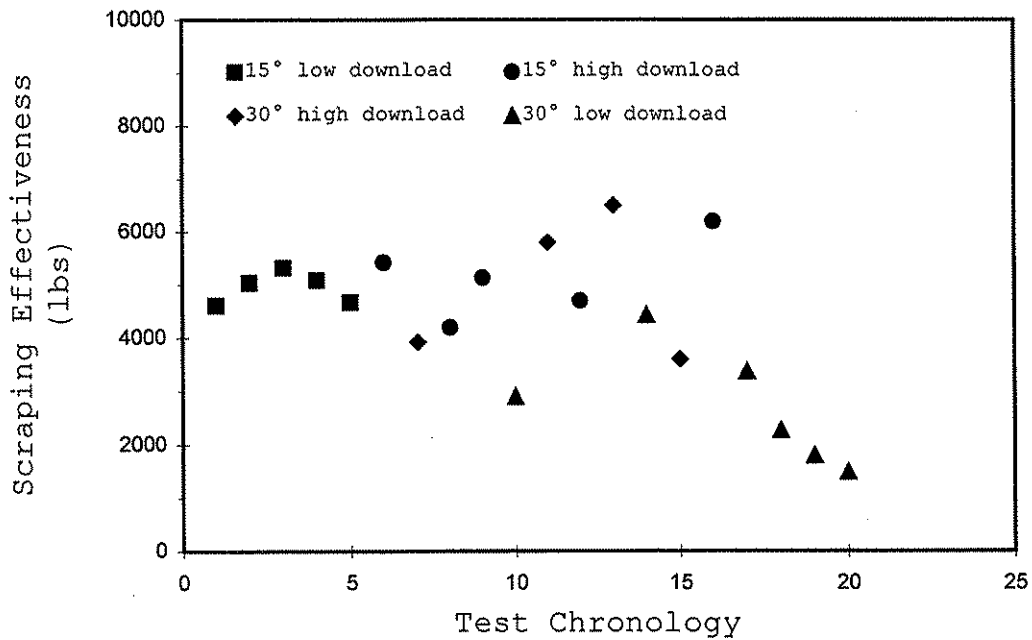


Figure 27 Effect of blade wear on scraping effectiveness for blade two tests

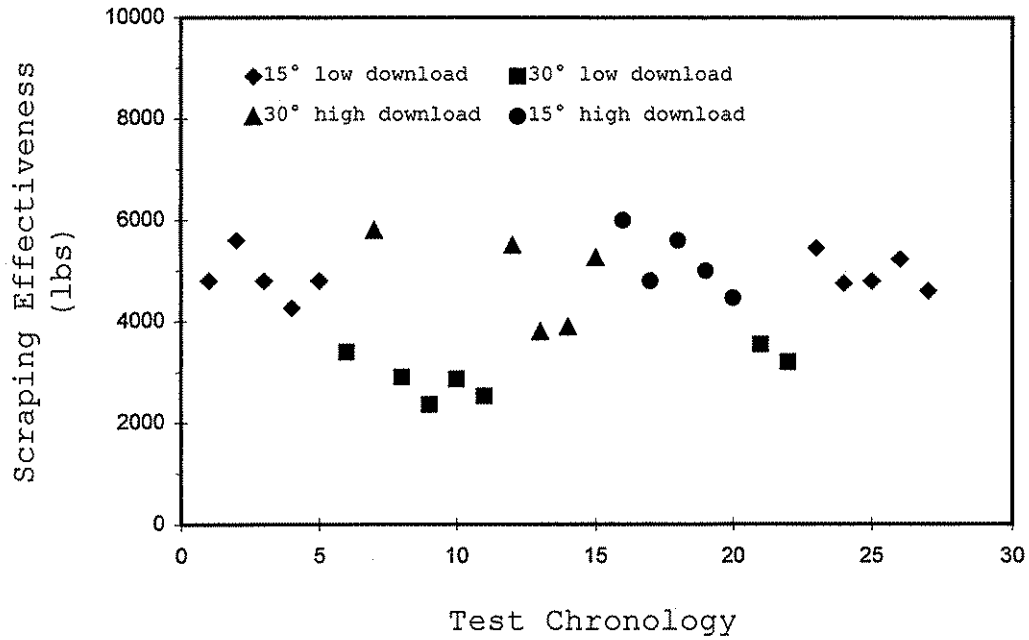


Figure 28 Effects of blade wear on scraping effectiveness for blade three tests

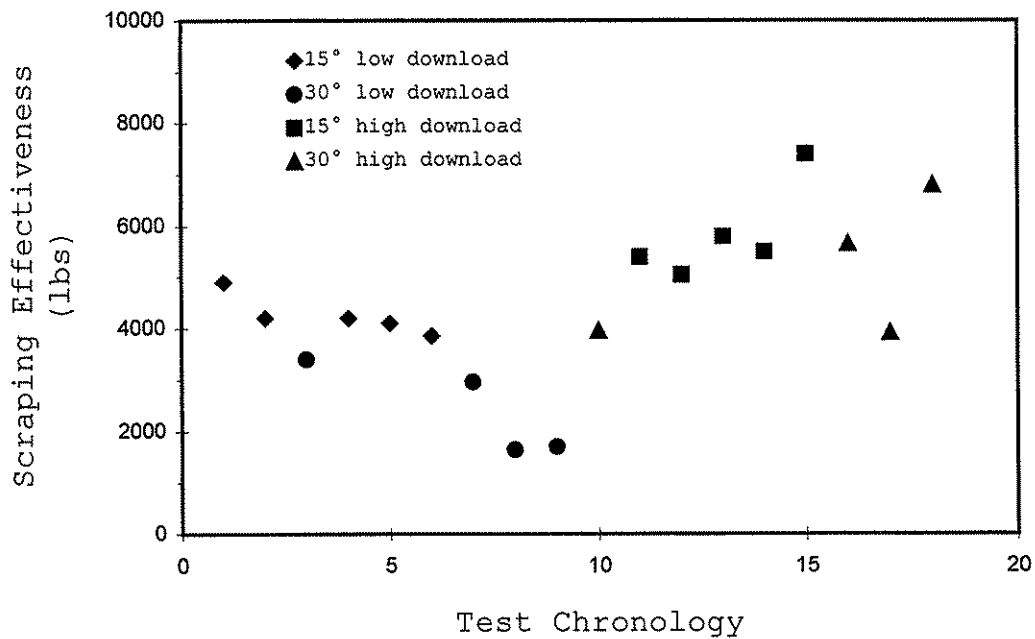


Figure 29 Effects of blade wear on scraping effectiveness for blade four tests



show a steady decline in magnitude. Secondly, of the four blades the test configuration that had the most consistent results was the 15° blade angle with a low download pressure. The test configuration that showed the most disparity among its results was the 30° blade angle with a high download pressure.

E. Modified Scraping Effectiveness Results. The previous section discussed the scraping effectiveness in terms of lbs per whole length of blade. Since blades two through four have serrated shapes, only a certain percentage of their cutting edges were in contact with the ice sheet. The modified scraping effectiveness will represent the scraping effectiveness in terms of lbs per length of blade in contact with the ice sheet, or lbs per unit scraping length. The modified scraping effectiveness of each blade will be calculated by increasing each blade's previous scraping effectiveness values by a certain percentage. This percentage increase is based on each blades serrated configuration.

The scraping effectiveness for blade one did not change because its cutting edge did not have a serrated shape. The scraping effectiveness values for blades two and three were increased by 66.7% since their serrated shapes consisted of a 1.5/1.0 teeth to gap ratio. Measuring the width of the teeth and gaps of blade three after the testing showed no significant change from the original values. Thus, it was safe to assume that the ratio was still 1.5/1.0 for blade three. The scraping effectiveness values for blade four will be increased by 25% because its serrated shape had a 1.0/1.5 teeth to gap ratio and because the blade configuration consisted of two cutting edges.

Figure 30 shows the modified scraping effectiveness for all blade configurations. Figure 31 shows the modified scraping effectiveness for all test configurations in descending order of effectiveness. The test configurations in Figure 31 are described on the X-axis by blade number, blade angle, and download pressure.

Figure 30 shows the effect blade angle has on the modified scraping effectiveness for all four blades. This figure shows the same correlation, a decrease in modified scraping effectiveness with an increase in blade angle, that was previously discussed for the scraping effectiveness.

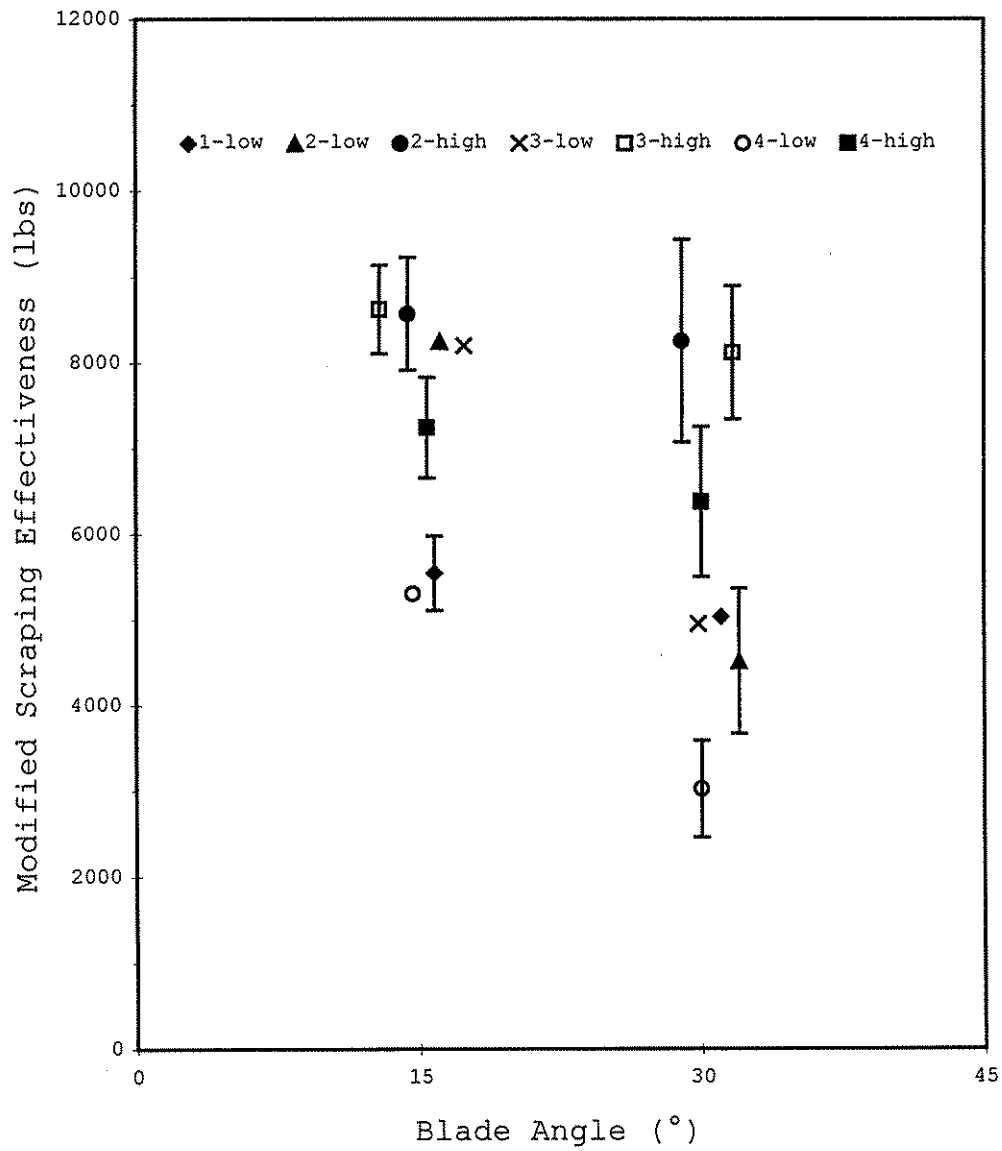


Figure 30 Modified scraping effectiveness for all blade configurations based on blade angle

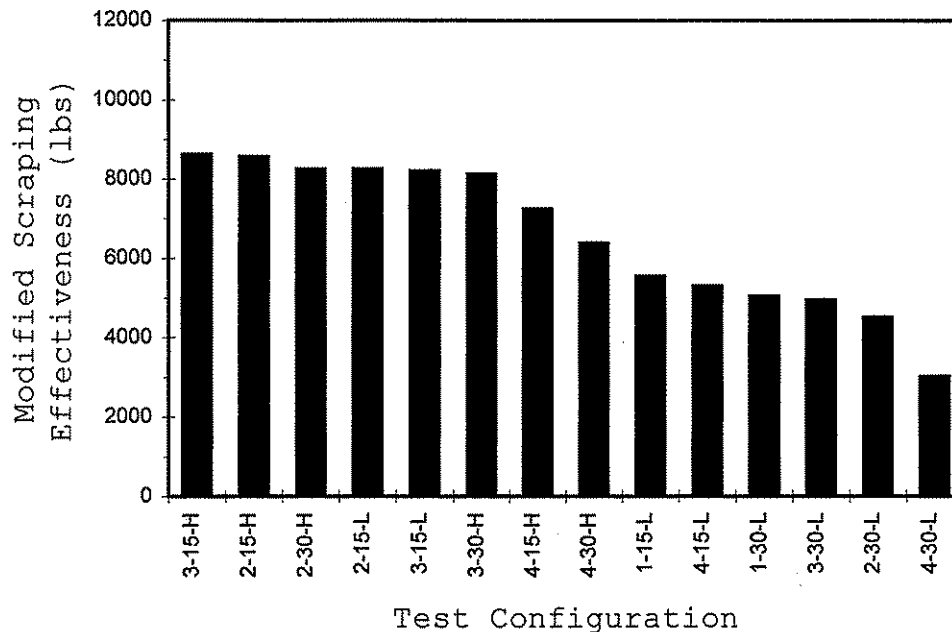


Figure 31 Modified scraping effectiveness for all test configurations based on decreasing order

Figure 31 shows that blade two and three have testing configurations that produce some of the larger modified scraping effectiveness values. Thus, these testing configurations of blade two and three should scrape the most ice from the ice sheet during a test. This theory is correct and will be explained further in detail later in the thesis.

F. Visual Results. Each blade's ability to remove ice can be seen visually. Figure 32 shows the typical ice sheet formed by the procedure described previously. Figures 33 and 34 show an ice sheet after a test using blade one. Figures 35 and 36 show the ice sheet after a test using blade two, and Figures 37 and 38 show the ice sheet after a test using blade three. Figures 39 and 40 show the ice sheet after a test using blade four.

Figure 33 and Figure 34 show the visual results for blade one. These figures show that only the left and right side of the ice sheet get scraped by blade one. This result was typical of every test with blade one. The amount of ice scraped varied between 0.13 in. and 0.25 in. The two sections of the ice sheet that were scraped line up perfectly with



Figure 32 Typical ice sheet prior to testing

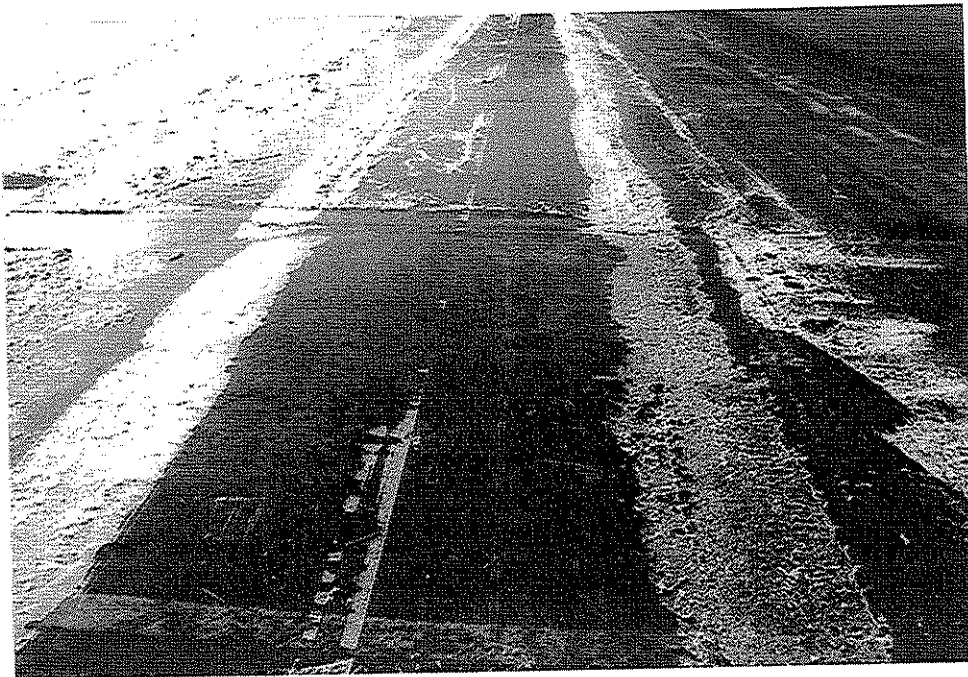


Figure 33 Ice sheet after testing with blade one

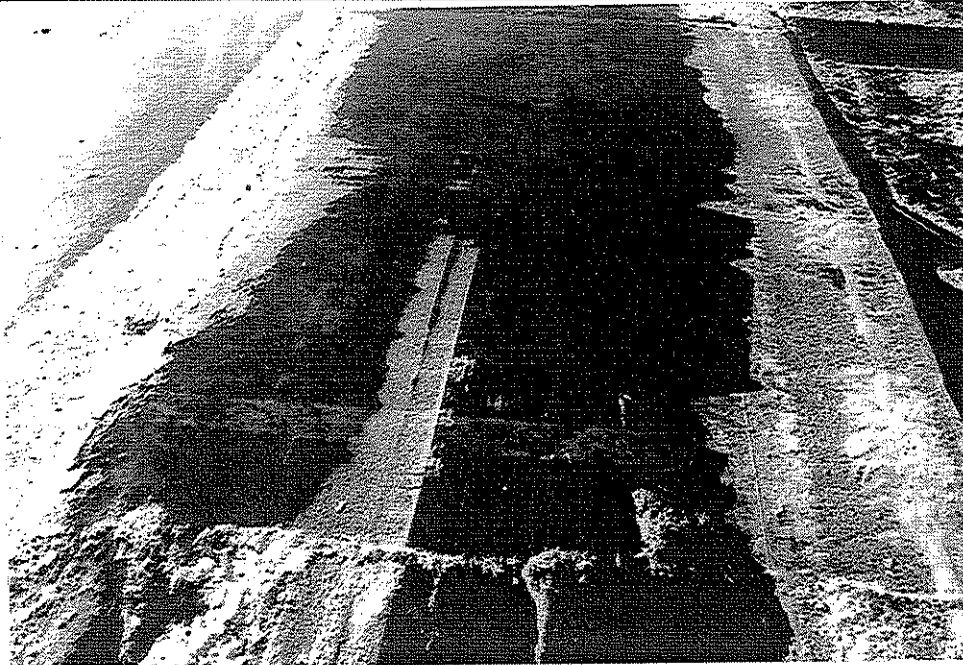


Figure 34 Ice sheet after testing with blade one

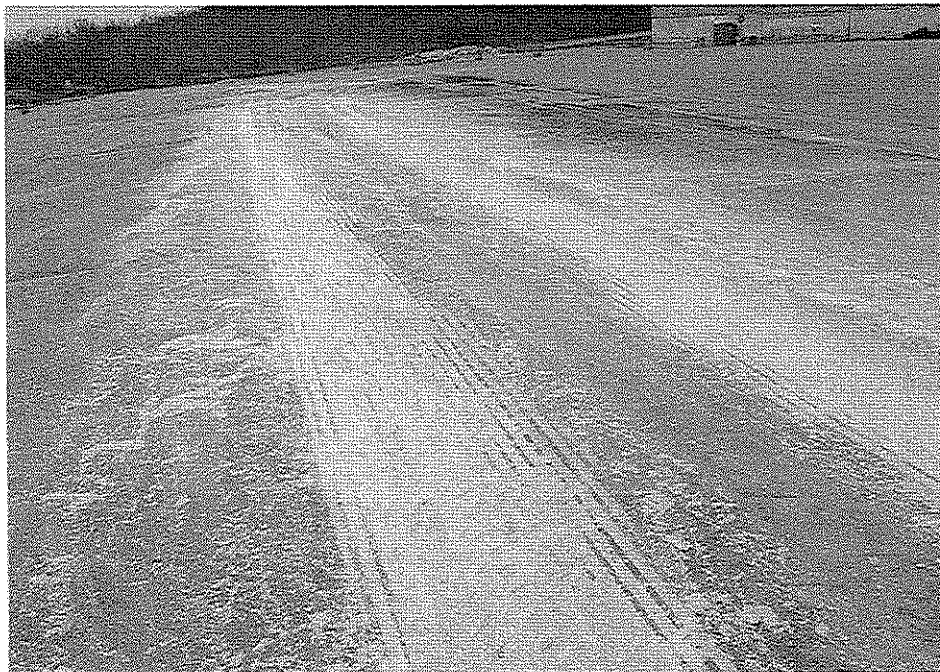


Figure 35 Ice sheet after testing with blade two



Figure 36 Ice sheet after testing with blade two



Figure 37 Ice sheet after testing with blade three



Figure 38 Ice sheet after testing with blade three



Figure 39 Ice sheet after testing with blade four



Figure 40 Ice sheet after testing with blade four

the location of the 3rd cylinders on the underbody. The middle of the blade must bow upwards (perhaps as a result of damage), because no ice was scraped in that region.

Figure 35 through Figure 38 show the visual results for blade two and blade three. These figures show grooves created in the ice sheet after testing with either blade. The depth of the grooves varied between 0.13 in. and 0.25 in., with a width slightly greater than the gaps in the blade. The figures show only the left and right side of the ice sheet being scraped. They were taken after the mold board had been accidentally bent out of shape. Tests conducted prior to the bent mold board resulted in the entire width of the ice sheet being scraped by blade two. Every test taken prior to the bent mold board produced grooves that were 0.13 in. to 0.25 in. in depth. After each test the grooves could not be seen visually because of the ice fragments lying across the entire ice sheet. The ice fragments size ranged between powder size to ice chunks as large as 1 x 0.25 in.

Figure 39 and Figure 40 show the visual results of blade four. These pictures were taken with an undamaged mold board. These results show how the grooves in the ice sheet occur across the entire path. The gaps in blade four were less than 0.25 in. but yet still produced grooves in the ice sheet. The grooves in the ice sheet were not as



consistent as the grooves produced by blades two and three. The width of the grooves varied between less than a 0.25 in. to approximately 1.5 in. This larger width can be produced by the blade nearest to the mold board not being in contact with the ice sheet. The vertical offset discussed earlier is only satisfactory for a certain blade angle. For these tests that blade angle was 23° , mean between 15° and 30° . Scraping ice at any other angle will result in one blade scraping more ice than the other blade.

IV. DESCRIPTION OF ICE SCRAPING

A. Introduction. The ideal method for removing ice from the road proposes to break the interface between the ice and the road, thus "peeling" the ice upward from the pavement. This ideal method has not been observed in these tests, nor in any laboratory scraping tests performed at the Iowa Institute of Hydraulic Research; instead the ice is pulverized into small pieces.

B. Standard Blade. Prior research (Nixon and Frisbie 1993) found that, when ice is being scraped by an underbody plow, there are two failure zones. This finding was verified by the tests conducted in this project. The two zones of failure are shown in Figure 41.

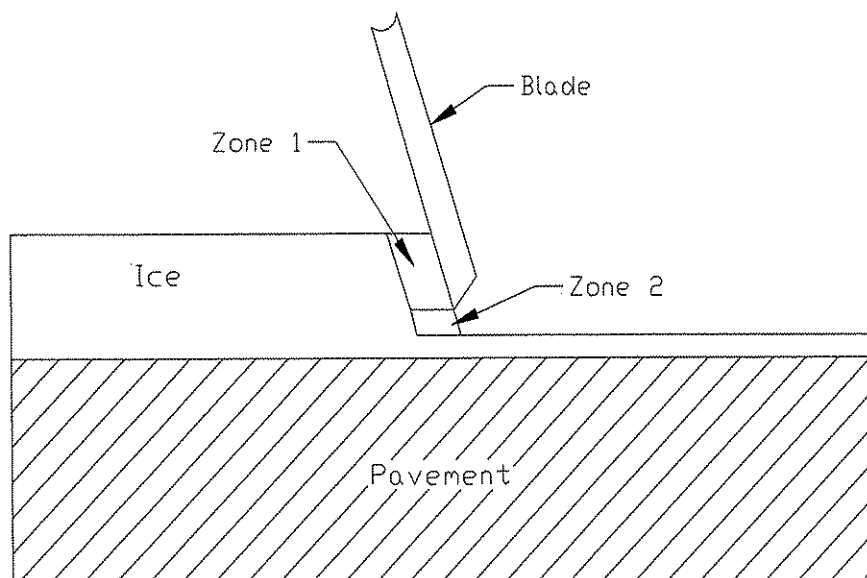


Figure 41 Two zones of ice failure produced by an underbody plow



The first zone represents ice that is fractured in front of the blade. This fracture is caused by the horizontal force applied to the ice. It causes ice fragments to be ejected into the air in front of blade, as can be seen in Figure 42.

The research conducted by Lieu and Mote (1984) also produced tests that resulted in ice fragments spraying out in front of the cutting edge. However, spraying of ice fragments only occurred for tests conducted on an ice thickness of 0.0078 in. (200 μm). Tests conducted on ice thickness of 0.0015 in. (38 μm) produced ice fragments which were continuous and well defined. The transition between continuous ice fragments and segmented ice fragments appeared to occur around an ice thickness of 0.0059 in. (150 μm).

The second zone represents ice compressed by the blade, then is ejected behind it. This zone is compressed by the vertical force being applied to the ice by the cutting edge. Figure 43 shows the underbody scraping ice and ice being ejected from zone two.

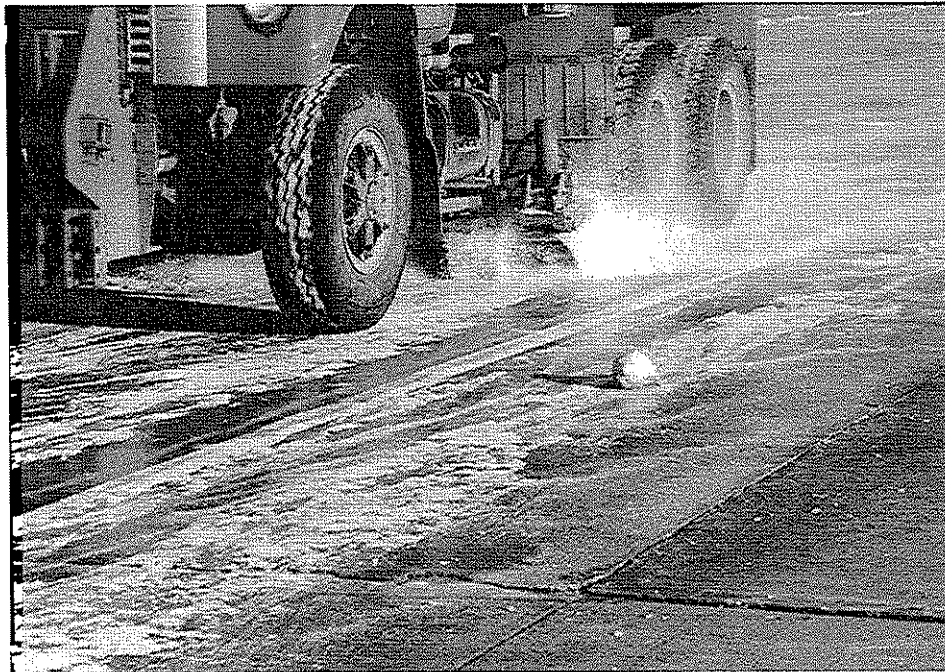


Figure 42 Close up of ice being ejected from zone one

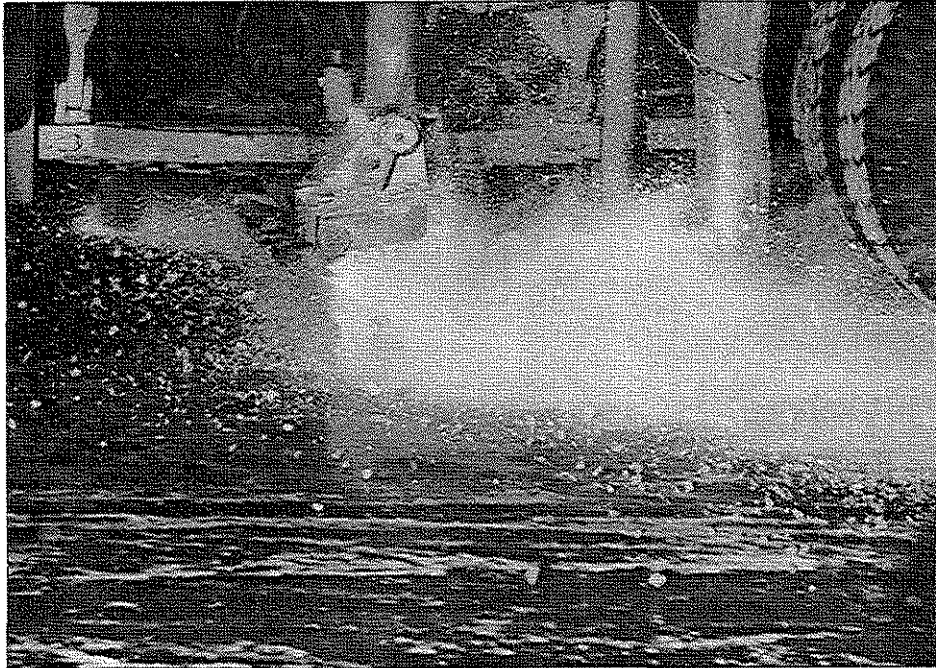


Figure 43 Close up of ice being ejected from zone two

C. Serrated Blade. Serrated blades experience a different type of fracturing due to the shape of the blade. The main difference between the two shapes is the serrated blades' inability to remove ice across the entire sheet of ice. Ice that lies in the path of the serrated gaps is not removed from the ice sheet.

Ice typically fractured in zones one and two, shown in Figure 41, is fractured in a similar manner. The serrated shape introduces a new zone of ice fracture. Grooves left behind in the ice sheet were smaller than the serrated gap, thus parts of the ice sheet must be fracturing alongside the serrated teeth of the blade. Zone three will be designated as the zone where ice fractures alongside the serrated teeth of the blade. Zone two and zone three are shown in Figure 44. This is only a preliminary description and requires further development.

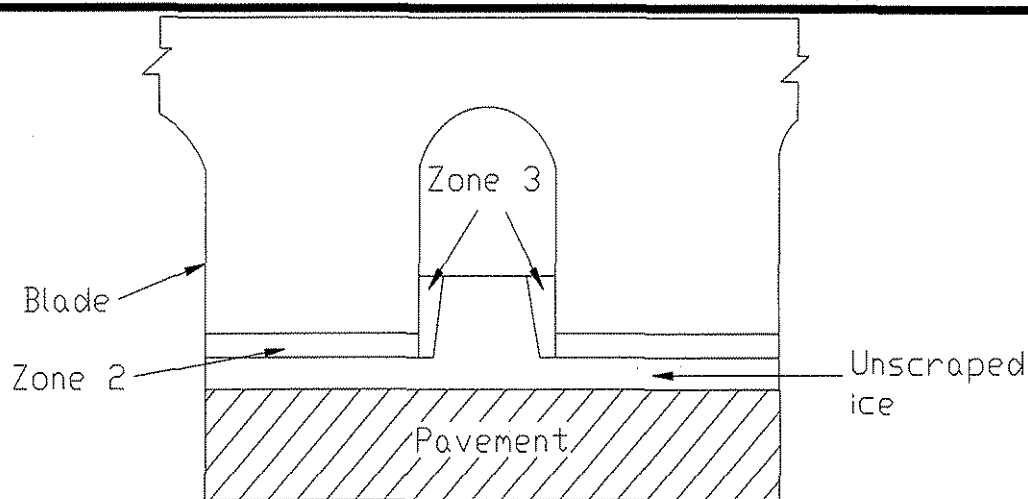


Figure 44 Front view of serrated blade showing zones two and three of fracture

V. DESCRIPTION OF IN-SERVICE TRUCKS

A. Truck Description. Tests were performed on two in-service 25 ton gross vehicle weight (GVW) dump trucks. These trucks were owned by the Iowa Department of Transportation and are used on the Interstate and major highways to remove ice or compacted snow from the roadway. Both trucks were fitted with an underbody plow which was essentially identical to the plow on the closed-road test truck.

B. Instrumentation. The trucks were each instrumented with a data acquisition system, pressure sensors and an inclinometer. The data acquisition system employed was a CardCorder data logger manufactured by Cranfield Impact Centre Ltd. The specifications of the CardCorder are:

- resolution 8 bit
- voltage range 0 to 10 volts
- max sample rate 1000 Hz
- memory card size 1 Mb
- dimensions 5 x 12 x 1.3 in

The CardCorder was located inside the cab and received power from an accessory line. All data collected by the CardCorder was recorded on a 1 Mb memory card. The memory card was then taken out of the CardCorder and downloaded to a PC by using a PCMCIA



card reader. The memory card was the size of a credit card but with a thickness of 0.12 in. The pressure sensors and inclinometer used on the in-service trucks were the same models that were used on the closed-road test truck and were calibrated in a similar manner.

VI. RESULTS AND DISCUSSION OF IN-SERVICE TRUCKS

A. Description of Data Collection. A summary of the results are listed in Table 1. A complete listing is given in Appendix C. A total of seven runs were conducted. A run represents a truck that has gone out on the Interstate 80 for approximately two to three hours before returning back to the shop to refuel. During the same run a truck may attempt to scrape ice from the roadway more than once. This is why multiple results may be listed in Table 1 for a given run.

Table 1 Results of in-service trucks

Run Number	Average Blade Angle (°)	Average Vertical Force (lbs)	Average Force Angle (°)	Average Horizontal Force (lbs)
1	38	7400	67	3200
1	40	10000	72	2700
1	38	8000	67	3500
1	38	10200	67	3200
1	43	13100	87	500
1	34	15500	85	1300
2	33	16000	73	4500
2	29	15000	67	6300
2	8	12000	60	7000
2	23	21000	69	7500
2	13	22000	69	7800
3	20	20000	72	7200
4	15	8000	55	5600
4	38	9600	67	4300
5	27	8500	63	3600
6	9	10000	57	6400
7	26	14000	75	3600
7	10	14000	68	5800
7	19	10000	60	5100



B. Comparison of Results. To determine if the in-service trucks produced similar results as those previously discussed in this report, the data obtained by the in-service trucks needed to be grouped into two different blade angles and two different download force groups. After arranging the data into these groups, the results from the in-service trucks can be compared to the closed-road tests.

Figure 45 shows the results of the data (averages and standard deviations) after being split into two different blade angle groups (15° and 38°). To ensure a significant break between the two blade angle groups, all tests with an average blade angle between 23° and 33° were not included in the results as shown in Figure 45. 15° and 38° represent the average of the remaining tests. Also shown in Figure 45 are the results from the closed-road tests.

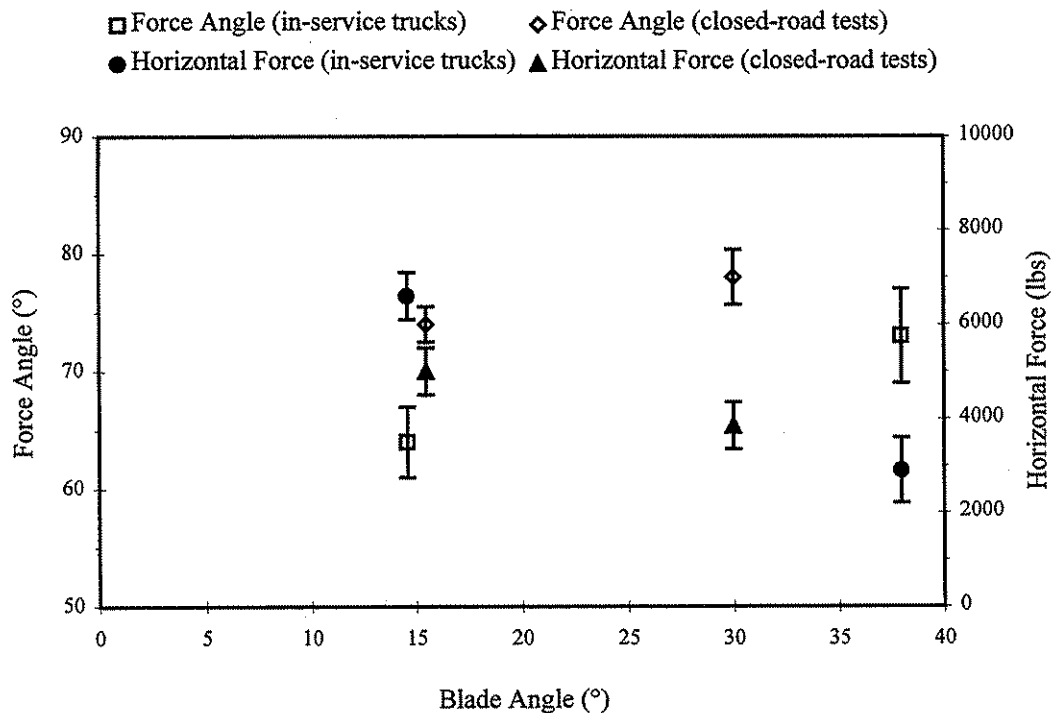
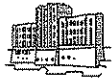


Figure 45 Results of blade angle effects

In the closed-road tests, it was shown that with a constant download force the horizontal force would decrease when the blade angle was increased. It was also shown



that the force angle would increase when the blade angle was increased. Figure 45 shows that these two trends also hold for the in-service trucks.

Figure 46 shows the effects of download force on the force angle for the results collected by the in-service trucks and the previously discussed results. For the in-service trucks the low download case had an average vertical force of 9,000 lbs and the high download case had an average of 20,000 lbs, as compared with 10,000 lbs and 23,000 lbs for the closed-road tests. Figure 46 shows that the force angle clearly increases from the low to the high download case for the in-service trucks. Again this mirrors the trend observed in the results of the closed-road tests.

Figure 47 shows the effects of download force on the horizontal force. Once again, the figure includes the results from both the in-service trucks and from the closed-road tests. Looking at the results obtained by the in-service trucks, it is apparent that the horizontal force increases when the download force is increased. Again, this correlation

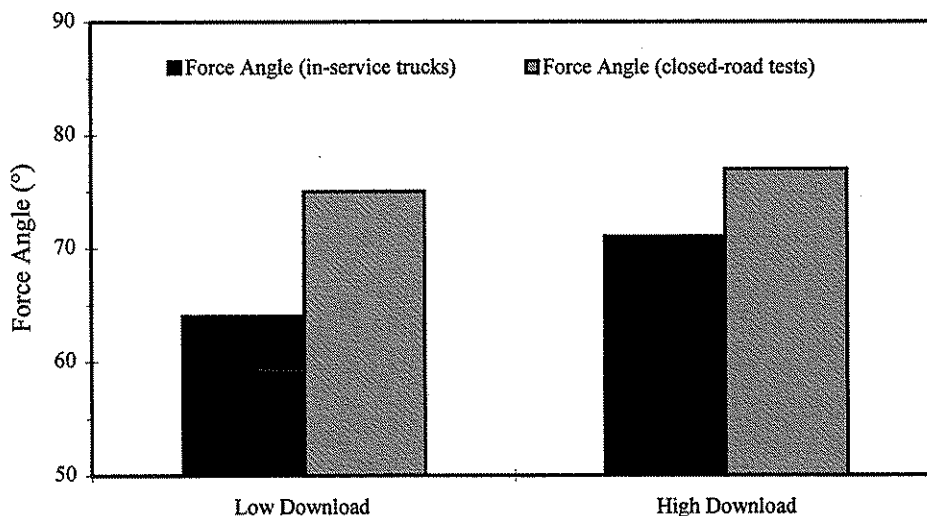


Figure 46 Download effects on force angle

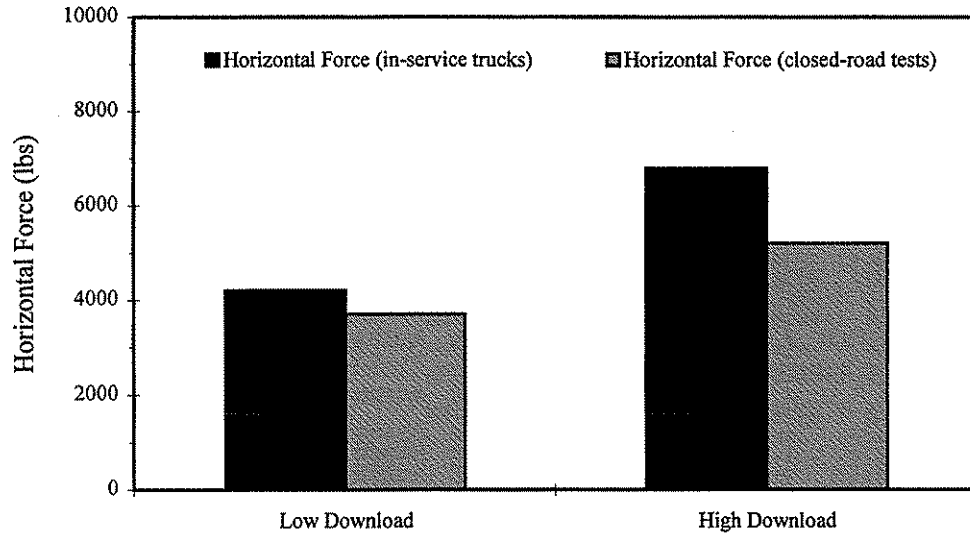


Figure 47 Download effects on horizontal force

also existed in the results of the closed-road tests.

Figures 45 through 47 make three things clear. First, the closed-road method reported previously gives results that are very similar to those obtained from the in-service trucks. This validates that research methodology described by Nixon and Smithson (1996). Second, both force angle and horizontal force increase with increasing download. Third, horizontal force decreases and force angle increase with increasing blade angle.

VII. CONCLUSIONS

A. Summary. The adverse effects of using road salt to clear snow and ice from roads have caught the public's attention. Today, the public is increasingly aware of the damages caused by polluting the environment with excessive amounts of chemicals. Groundwater, roadside vegetation, and automobiles have all been adversely affected by the use of road salt over the years. Since road salt is a very cheap method of deicing, developing a viable alternate method for removing snow and ice is a difficult task. Reducing the amount of road salt applied to the roadway is a more realistic goal than



ceasing to use road salt altogether. One method for attaining the goal is to develop more effective ice-scraping blades for use on snow-plow trucks.

The purpose of the closed-road tests was to determine an optimal configuration of blade cutting edge to maximize the amount of ice scraped from road pavement, for given energy limitations. The main factors determining optimal blade configuration are blade angle and download pressure. The purpose of the in-service trucks was to collect real life ice scraping data and compare it to the data collected in the closed-road tests.

From the work performed in this study, the following conclusions can be made:

1. The testing method developed can easily be applied to other underbody plows fitted to different trucks to determine optimally efficient and effective blades for scraping ice from road.
2. Force angle and scraping effectiveness (see page 15) are useful parameters for analyzing the results of blade cutting edge performance. They describe how well a cutting edge removes ice while also indicating the degree of control that the truck operator has over the truck. The optimal results of a test would be a maximized scraping effectiveness with a minimized force angle.
3. Four blades were tested and compared (see Figures 5 through 7). Blade one was tested previously (Nixon and Frisbie 1993); blades two through four were tested for the first time. When comparing their performances together, blades two through four shared some common trends. All three blades demonstrated maximum scraping effectiveness when the test configuration consisted of a 15° blade angle and a high download pressure. Also, all three blades demonstrated minimum force angle with a test configuration of 15° blade angle and a low download pressure. It is interesting to note that these conditions are well within the range used by the experienced plow operators in the in-service part of the study.
4. Tests conducted on blades two and three produced grooves in the ice sheet. The grooves of remnant ice were larger than the gaps between the teeth of the blade (see Figure 44). Tests on blade four also left grooves in the ice, but these were not as deep as the grooves produced by blades two and three.
5. Excessive wear on a blade affected the blade's effectiveness to scrape ice.



The effects of wear appeared to be minimized when the blade angle was changed between tests (see Figure 21).

6. The results of all four blades showed air temperature having no effect on the force angle and scraping effectiveness.

7. The testing method developed for the closed-road tests was successfully applied to other underbody plows fitted to different trucks. Accordingly, the forces experienced by a cutting edge while scraping ice can be determined relatively easily.

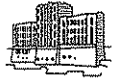
B. Future Research. The results of this study provide insights for future research in the area of ice removal. Research in the following areas could help produce a more efficient scraping method in removing ice:

1. Providing instantaneous feedback of the blade angle and download pressure to the truck operator while in the field. This would help the truck operator to maintain an optimum ice scraping configuration at all times.

2. Controlling the blade angle and download pressure automatically through the use of a computerized control system. By programming a computer to calculate the current horizontal force the system could automatically adjust the blade angle and download pressure when the horizontal force dropped below a specified value.

3. Future research in this field could determine the effect that other parameters may have on the ice scraping process. Future research could include:

- Conducting a series of tests to determine how the horizontal force changes with different pavement types.
- Conducting a series of tests to determine the effects that pretreating ice with chemicals may have on the horizontal force.
- Conducting a series of tests to clarify the relationship between the magnitude of the horizontal force to the amount of ice removed from the pavement.
- Conducting a series of tests in the field to determine the extent to which the superior performance found herein for serrated blades carries over into field situations.



-
- Conducting a series of tests to develop a composite material that would be more resilient to wear than the standard materials used in the field today.

The method used in this study can hopefully lead to the development of cutting edges that can successfully remove ice from the pavement without requiring large amounts of energy. Such edges would reduce chemical usage, and increase operator control and safety. Additional sensor developments, up to some form of computer control of the plowing process, could also bring substantial safety and operational benefits.

C: Implementation. The following steps are proposed for implementation of the findings of this study.

1. That the Iowa DOT, and Cities and Counties within Iowa use serrated cutting edges on their underbody plows, for use when plowing ice or compacted snow. As a first step in this implementation, an evaluation process should be used whereby the three different configurations tested here can be tried in the field and evaluated by different organizations to determine how well they meet the needs of the various agencies. Of the three serrated configurations tested in this study, the third configuration (blade 4, with two overlapping serrated cutting edges) showed the most promise, and should receive most attention in testing.
2. That the Iowa DOT, and Cities and Counties within Iowa consider a program to instrument their underbody plows so that download, blade angle, and horizontal cutting force can be displayed in the cab. Such displays could be very useful for training and have the potential to improve plowing performance.
3. That the Iowa DOT, and Cities and Counties within Iowa consider developing an expert system based computer control for underbody plows, which could handle all underbody plowing duties for truck operators. Some work is needed to develop a suitable control algorithm for this, but sufficient data are now available that the system can be developed if deemed of interest.



With regard to technology transfer, preliminary results from this study were presented at the 4th International Symposium on Snow Removal and Ice Control Technology in Reno, Nevada, August, 1996. Details of this report (including the abstract) will be posted on the snow and ice mailing list (snow-ice@list.uiowa.edu) which has about fifty e-mail subscribers from around the world. It is expected that two Journal papers on this work will also be published.



REFERENCES

Lieu, D.K., Mote Jr., C.D. (1984) "Experiments in the Machining of Ice at Negative Rake Angles", Journal of Glaciology, Vol. 30, No. 104, 1984.

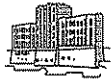
Nixon, W.A. and Frisbie, T.R. (1993). "Field Measurements of Plow Loads During Ice Removal Operations", Iowa Department of Transportation Project HR 334, Iowa Institute of Hydraulic Research, Technical Report Number 365.

Nixon, W.A. and Smithson, L.D. (1996). "Methodology for Conducting Research into Winter Highway Maintenance", Fourth International Symposium on Snow Removal and Ice Control Technology, Transportation Research Board, National Research Council, Washington, D.C., Paper A-10, Volume 1, August 1996.



APPENDIX A

Closed-road results



Test No.	Date/ Test Conditions		Vertical Force (kip)	Horizontal Force (kip)	Blade Angle (degree)	Force Angle (degree)
1	1/18/96 30° low Blade 1 Temp. 10°F	max	14.8	7.4	33	86
		min	9.3	0.7	16	60
		mean	12.4	5.3	27	67
		stdev	0.9	0.9	4.5	--
2	1/18/96 15° low Blade 1 Temp. 10° F	max	19.6	11.6	22	75
		min	10.0	4.5	8	54
		mean	15.4	6.2	12	68
		stdev	1.5	0.5	3	--
3	1/18/96 15° low Blade 1 Temp. 10°F	max	17.1	7.1	30	78
		min	9.5	3.3	16	54
		mean	13.0	5.4	18	68
		stdev	1.6	0.5	2	--
4	1/18/96 30° low Blade 1 Temp. 0°F	max	15.2	5.9	35	86
		min	9.5	0.9	25	60
		mean	11.5	4.0	30	73
		stdev	1.4	0.8	2	--
5	1/18/96 15° low Blade 1 Temp. -4°F	max	21.2	7.9	20	76
		min	10.0	4.3	8	54
		mean	16.0	6.3	16	69
		stdev	1.7	0.5	3	--
6	1/18/96 30° low Blade 1 Temp. -4°F	max	18.7	7.4	28	84
		min	9.0	1.2	18	56
		mean	11.7	4.9	26	69
		stdev	1.8	0.9	4	--
7	1/20/96 15° low Blade 3 Temp. 12°F	max	18.2	7.7	30	80
		min	8.2	3.3	12	56
		mean	14.1	4.8	18	72
		stdev	1.8	0.6	3	--
8	1/20/96 15° low Blade 3 Temp. 12°F	max	18.0	10.0	25	76
		min	8.9	4.1	11	48
		mean	13.3	5.6	17	67
		stdev	1.5	0.7	2	--
9	1/20/96 15° low Blade 3 Temp. 12°F	max	18.0	11.8	27	79
		min	10.6	3.1	10	52
		mean	14.5	4.8	17	72
		stdev	1.4	1.1	4	--



Test No.	Date/ Test Conditions		Vertical Force (kip)	Horizontal Force (kip)	Blade Angle (degree)	Force Angle (degree)
10	1/20/96 15° low Blade 3 Temp. 12°F	max	17.8	5.3	22	80
		min	8.9	3.0	7	61
		mean	13.4	4.3	15	73
		stdev	1.4	0.4	3	--
11	1/20/96 15° low Blade 3 Temp. 12°F	max	17.9	5.7	22	79
		min	7.2	3.2	9	54
		mean	12.2	4.8	15	69
		stdev	2.0	0.4	3	--
12	1/20/96 30° low Blade 3 Temp. 10°F	max	13.8	3.6	38	86
		min	7.4	1.1	23	67
		mean	10.7	2.5	29	77
		stdev	1.2	0.5	2	--
13	1/20/96 30° low Blade 3 Temp. 10°F	max	16.0	9.1	35	86
		min	9.9	1.0	17	52
		mean	13.3	3.4	28	77
		stdev	1.2	1.1	3	--
14	1/20/96 30° low Blade 3 Temp. 10°F	max	12.7	5.6	38	84
		min	5.7	1.3	26	50
		mean	10.6	2.9	31	75
		stdev	1.2	0.7	2	--
15	1/20/96 30° low Blade 3 Temp. 10°F	max	12.0	4.5	34	86
		min	5.7	0.8	23	58
		mean	9.6	2.4	30	77
		stdev	0.9	0.5	2	--
16	1/20/96 30° low Blade 3 Temp. 10°F	max	14.8	5.6	42	87
		min	9.4	0.6	27	63
		mean	11.9	2.9	34	77
		stdev	0.9	0.7	3	--
17	1/20/96 30° high Blade 3 Temp. 10°F	max	20.8	10.8	34	85
		min	10.4	1.9	24	51
		mean	17.3	5.8	30	74
		stdev	1.6	1.9	2	--
18	1/21/96 15° high Blade 3 Temp. 10°F	max	25.6	10.1	26	83
		min	20.0	2.9	12	65
		mean	23.2	6.0	19	76
		stdev	1.1	1.1	3	--



Test No.	Date/ Test Conditions		Vertical Force (kip)	Horizontal Force (kip)	Blade Angle (degree)	Force Angle (degree)
19	1/21/96	max	22.1	7.6	28	85
	15° high	min	15.0	1.6	6	67
	Blade 3	mean	18.9	4.8	16	76
	Temp. 10°F	stdev	1.3	0.9	4	--
20	1/21/96	max	23.7	9.4	32	87
	15° high	min	12.4	0.9	5	58
	Blade 3	mean	19.0	5.6	19	76
	Temp. 10°F	stdev	1.9	1.8	6	--
21	1/21/96	max	24.9	8.5	26	85
	15° high	min	12.1	1.7	1	60
	Blade 3	mean	17.6	5.0	13	75
	Temp. 10°F	stdev	1.9	1.1	4	--
22	1/21/96	max	20.5	7.6	24	85
	15° high	min	14.2	1.7	6	66
	Blade 3	mean	17.1	4.5	17	76
	Temp. 10°F	stdev	1.1	1.0	4	--
23	1/21/96	max	25.8	7.5	31	85
	30° high	min	20.0	2.0	18	71
	Blade 3	mean	23.9	5.5	28	77
	Temp. 12°F	stdev	0.8	0.9	2	--
24	1/21/96	max	21.7	5.9	33	87
	30° high	min	15.0	0.7	19	71
	Blade 3	mean	18.6	3.8	25	79
	Temp. 12°F	stdev	1.1	1.0	3	--
25	1/21/96	max	20.3	6.3	37	88
	30° high	min	9.6	0.6	10	56
	Blade 3	mean	16.4	3.9	28	77
	Temp. 12°F	stdev	1.5	0.9	3	--
26	1/21/96	max	19.6	8.2	39	81
	30° high	min	11.1	2.8	23	56
	Blade 3	mean	16.4	5.2	32	72
	Temp. 12°F	stdev	1.6	1.0	3	--
27	1/23/96	max	15.8	5.1	36	82
	30° low	min	9.1	2.0	18	67
	Blade 3	mean	13.8	3.6	31	76
	Temp. 22°F	stdev	0.9	0.4	2	--



Test No.	Date/ Test Conditions		Vertical Force (kip)	Horizontal Force (kip)	Blade Angle (degree)	Force Angle (degree)
28	1/23/96 30° low Blade 3 Temp. 22°F	max	13.2	4.2	27	79
		min	8.3	2.6	15	65
		mean	11.2	3.2	24	74
		stdev	0.8	0.3	2	--
29	1/25/96 15° low Blade 1 Temp. 22°F	max	16.1	6.3	21	74
		min	9.9	4.3	14	60
		mean	11.7	5.3	18	66
		stdev	1.0	0.2	2	--
30	1/25/96 15° low Blade 1 Temp. 22°F	max	16.7	5.5	25	75
		min	9.9	4.2	12	61
		mean	10.2	5.1	16	63
		stdev	0.7	0.2	3	--
31	1/25/96 15° low Blade 1 Temp. 22°F	max	19.3	6.2	25	81
		min	10.0	2.3	12	63
		mean	13.4	4.2	18	73
		stdev	1.4	4.5	3	--
32	1/25/96 15° low Blade 3 Temp. 24°F	max	15.5	6.2	22	73
		min	9.8	4.5	14	58
		mean	12.1	5.5	18	66
		stdev	0.8	0.2	1	--
33	1/25/96 15° low Blade 3 Temp. 24°F	max	20.0	5.9	23	78
		min	11.0	3.7	14	65
		mean	15.1	4.8	17	73
		stdev	1.2	0.3	2	--
34	1/25/96 15° low Blade 3 Temp. 24°F	max	16.4	6.0	25	78
		min	9.8	3.2	15	61
		mean	12.3	4.8	18	70
		stdev	1.4	0.4	2	--
35	1/25/96 15° low Blade 3 Temp. 22°F	max	18.4	5.9	23	78
		min	9.9	3.1	12	62
		mean	11.9	4.6	16	69
		stdev	1.6	0.3	2	--
36	1/25/96 15° low Blade 3 Temp. 22°F	max	21.7	6.4	31	79
		min	9.9	2.9	11	60
		mean	13.2	5.2	18	68
		stdev	1.1	0.4	3	--



Test No.	Date/ Test Conditions		Vertical Force (kip)	Horizontal Force (kip)	Blade Angle (degree)	Force Angle (degree)
37	2/2/96 15° low Blade 2 Temp. -17°F	max	20.0	9.1	26	82
		min	10.3	2.5	12	50
		mean	15.2	4.9	17	73
		stdev	1.8	0.8	4	--
38	2/2/96 15° low Blade 2 Temp. -17°F	max	17.2	9.4	29	82
		min	10.3	2.4	11	50
		mean	13.2	5.0	16	70
		stdev	1.4	1.2	5	--
39	2/2/96 15° low Blade 2 Temp. -17°F	max	20.4	8.4	21	79
		min	10.5	3.4	13	52
		mean	1.4	5.3	17	70
		stdev	1.5	0.8	2	--
40	2/2/96 15° low Blade 2 Temp. -17°F	max	20.4	5.7	22	81
		min	10.5	3.2	13	61
		mean	12.9	5.1	17	69
		stdev	1.3	0.4	2	--
41	2/2/96 15° low Blade 2 Temp. -17°F	max	20.6	5.7	20	80
		min	10.4	3.4	13	61
		mean	14.3	4.7	16	72
		stdev	1.7	0.4	2	--
42	2/3/96 15° high Blade 2 Temp. -10°F	max	24.0	10.7	22	81
		min	10.6	3.5	14	54
		mean	18.4	5.4	17	74
		stdev	1.9	1.1	2	--
43	2/3/96 15° high Blade 2 Temp. -10°F	max	24.9	5.9	23	85
		min	10.3	2.1	14	61
		mean	19.8	4.2	18	78
		stdev	2.3	0.6	3	--
44	2/3/96 15° high Blade 2 Temp. -10°F	max	27.8	10.8	26	86
		min	11.1	1.6	15	60
		mean	21.8	5.1	20	79
		stdev	2.8	2.0	2	--
45	2/3/96 15° high Blade 2 Temp. 3°F	max	24.2	7.3	25	87
		min	10.2	1.2	16	61
		mean	19.2	4.7	21	77
		stdev	1.9	1.0	2	--



Test No.	Date/ Test Conditions		Vertical Force (kip)	Horizontal Force (kip)	Blade Angle (degree)	Force Angle (degree)
46	2/3/96 15° high Blade 2 Temp. 3°F	max	31.3	11.0	24	80
		min	10.1	3.0	8	54
		mean	18.9	6.3	17	72
		stdev	8.3	0.9	4	--
47	2/3/96 30° high Blade 2 Temp. 10°F	max	23.8	8.1	27	85
		min	11.9	1.8	21	68
		mean	19.4	3.9	24	79
		stdev	1.8	1.0	1	--
48	2/3/96 30° low Blade 2 Temp. 10°F	max	17.1	4.8	34	87
		min	10.2	0.9	26	66
		mean	12.7	2.9	28	78
		stdev	1.7	0.6	2	--
49	2/4/96 30° high Blade 2 Temp. 3°F	max	30.5	9.8	31	84
		min	21.9	3.1	23	72
		mean	27.8	5.8	26	78
		stdev	1.1	1.1	2	--
50	2/4/96 30° high Blade 2 Temp. 3°F	max	29.0	14.3	29	85
		min	12.2	2.3	17	52
		mean	23.1	6.5	24	76
		stdev	2.4	2.2	3	--
51	2/4/96 30° high Blade 2 Temp. 3°F	max	21.6	7.2	36	88
		min	10.2	0.4	29	67
		mean	17.0	3.6	32	79
		stdev	1.6	1.0	1	--
52	2/4/96 30° low Blade 2 Temp. 3°F	max	20.3	7.9	36	81
		min	10.6	2.6	29	61
		mean	14.9	4.4	32	75
		stdev	1.5	1.1	2	--
53	2/4/96 30° low Blade 2 Temp. 3°F	max	14.1	4.7	33	81
		min	10.1	2.0	27	66
		mean	11.3	3.4	29	74
		stdev	0.8	0.4	1	--
54	2/4/96 30° low Blade 2 Temp. 3°F	max	16.9	4.1	32	86
		min	10.3	1.0	28	69
		mean	14.0	2.3	30	81
		stdev	1.3	0.4	1	--



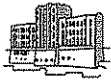
Test No.	Date/ Test Conditions		Vertical Force (kip)	Horizontal Force (kip)	Blade Angle (degree)	Force Angle (degree)
55	2/4/96	max	18.2	6.0	32	90
	30° low	min	10.1	0.9	27	62
	Blade 2	mean	15.5	1.8	29	84
	Temp. 3°F	stdev	1.8	0.6	1	--
56	2/4/96	max	17.7	3.3	29	87
	30° low	min	10.1	0.7	24	72
	Blade 2	mean	15.0	1.5	26	85
	Temp. 3°F	stdev	1.4	0.4	1	--
57	2/12/96	max	18.9	6.1	24	79
	15° low	min	9.9	3.4	15	58
	Blade 4	mean	14.0	4.9	19	71
	Temp. 26°F	stdev	1.8	0.4	2	--
58	2/12/96	max	18.6	6.2	33	86
	15° low	min	9.8	1.1	14	61
	Blade 4	mean	14.1	4.2	19	74
	Temp. 26°F	stdev	1.7	0.6	3	--
59	2/12/96	max	18.4	5.5	24	81
	15° low	min	9.8	2.6	9	61
	Blade 4	mean	11.2	4.2	15	70
	Temp. 26°F	stdev	1.7	0.4	2	--
60	2/12/96	max	16.2	8.3	28	82
	15° low	min	9.7	1.7	10	50
	Blade 4	mean	10.7	4.1	13	69
	Temp. 26°F	stdev	1.2	0.4	3	--
61	2/12/96	max	16.9	4.8	23	81
	15° low	min	9.8	2.6	9	65
	Blade 4	mean	10.8	3.9	14	70
	Temp. 26°F	stdev	1.3	0.3	2	--
62	2/12/96	max	19.8	7.9	40	87
	30° low	min	10.0	0.9	18	56
	Blade 4	mean	14.4	3.4	27	78
	Temp. 26°F	stdev	2.1	1.2	6	--
63	2/12/96	max	13.2	4.8	35	84
	30° low	min	9.7	1.4	28	65
	Blade 4	mean	10.2	3.0	32	74
	Temp. 26°F	stdev	0.6	0.7	1	--



Test No.	Date/ Test Conditions		Vertical Force (kip)	Horizontal Force (kip)	Blade Angle (degree)	Force Angle (degree)
64	2/12/96 30° low Blade 4 Temp. 26°F	max	15.4	3.7	36	89
		min	9.8	0.2	29	70
		mean	13.1	1.6	32	83
		stdev	1.0	0.5	1	--
65	2/12/96 30° low Blade 4 Temp. 26°F	max	14.6	3.1	33	88
		min	9.7	0.6	28	72
		mean	12.4	1.7	31	83
		stdev	1.0	0.4	1	--
66	2/13/96 15° high Blade 4 Temp. 25°F	max	23.9	9.0	24	82
		min	17.8	3.3	12	66
		mean	22.0	5.3	16	77
		stdev	0.9	0.8	3	--
67	2/13/96 15° high Blade 4 Temp. 25°F	max	23.5	6.3	18	80
		min	16.9	3.4	10	72
		mean	20.0	5.0	12	76
		stdev	1.1	0.5	2	--
68	2/13/96 15° high Blade 4 Temp. 25°F	max	21.7	13.9	28	83
		min	13.7	2.1	8	48
		mean	18.8	5.8	14	74
		stdev	1.7	1.7	6	--
69	2/13/96 15° high Blade 4 Temp. 25°F	max	24.8	11.4	27	86
		min	16.3	1.4	10	58
		mean	20.6	5.5	16	76
		stdev	1.4	1.1	3	--
70	2/13/96 15° high Blade 4 Temp. 25°F	max	26.5	15.5	32	78
		min	12.4	4.6	8	45
		mean	20.0	7.4	15	71
		stdev	3.5	2.3	6	--
71	2/13/96 30° high Blade 4 Temp. 25°F	max	25.7	7.6	30	87
		min	2.5	2.0	15	72
		mean	23.0	4.0	25	81
		stdev	2.3	1.5	5	--
72	2/13/96 30° high Blade 4 Temp. 25°F	max	24.0	13.4	30	86
		min	22.0	1.4	25	58
		mean	22.8	5.7	27	77
		stdev	0.7	1.6	1	--



Test No.	Date/ Test Conditions		Vertical Force (kip)	Horizontal Force (kip)	Blade Angle (degree)	Force Angle (degree)
73	2/13/96 30° high Blade 4 Temp. 25°F	max	27.8	11.8	28	88
		min	26.4	0.8	24	67
		mean	27.0	3.9	25	83
		stdev	3.2	1.7	1	--
74	2/13/96 30° high Blade 4 Temp. 25°F	max	26.4	12.8	28	90
		min	25.0	0.2	23	63
		mean	25.7	6.8	25	80
		stdev	0.3	3.2	1	--



APPENDIX B

Method for determining horizontal force



This appendix will explain how the horizontal load is determined from the following variables:

- blade angle
- vertical download
- pressure in the 3rd cylinder

The horizontal force is calculated by summing forces about a pin located on the underbody. For future reference this pin will be designated as pin A. The pin that connects the 3rd cylinder to the mold board will be designated as pin B. Figure 45 shows the location of these pins relative to the vertical force and horizontal force.

A new angle will be designated as β (beta) and will represent the angle the 3rd cylinder makes with the vertical. Lastly, α (alpha) will represent the angle that is formed by pin A, pin B and the vertical extending from pin B. Figure 46 shows α , β and $F(1)$ (force in 3rd cylinder) as well as the horizontal force and vertical force.

In order to sum forces about pin A, three moment arms must be known. The first two are very easily determined by geometry, they are designated as "X" and "Z", for the vertical and horizontal force, respectively. The distance "X" multiplied by the vertical force represents the moment produced by the vertical force about pin A. This can also be said for "Z" and the horizontal force. These two distances are known values for any given blade angle. Both of these distances, "X" and "Z", are functions of blade angle and blade height. These distances are plotted in Figure 47 for a six inch blade. The negative value for "X" represents the vertical force being to the left of pin A. This negative value occurs when the blade angle is near 6° . Thus for any given blade angle, the moment produced about pin A by the vertical and horizontal forces can be determined.

The third moment arm is not as easily determined as the other two. The distance between pin A and pin B was determined by analyzing the geometry of the mold board; later it was rechecked by measuring the distance directly from the truck. The distance between pin A and pin B was determined to be 5.8 in. Pin B is rigidly attached to the mold board, thus any changes in the blade angle will also change the position of pin B

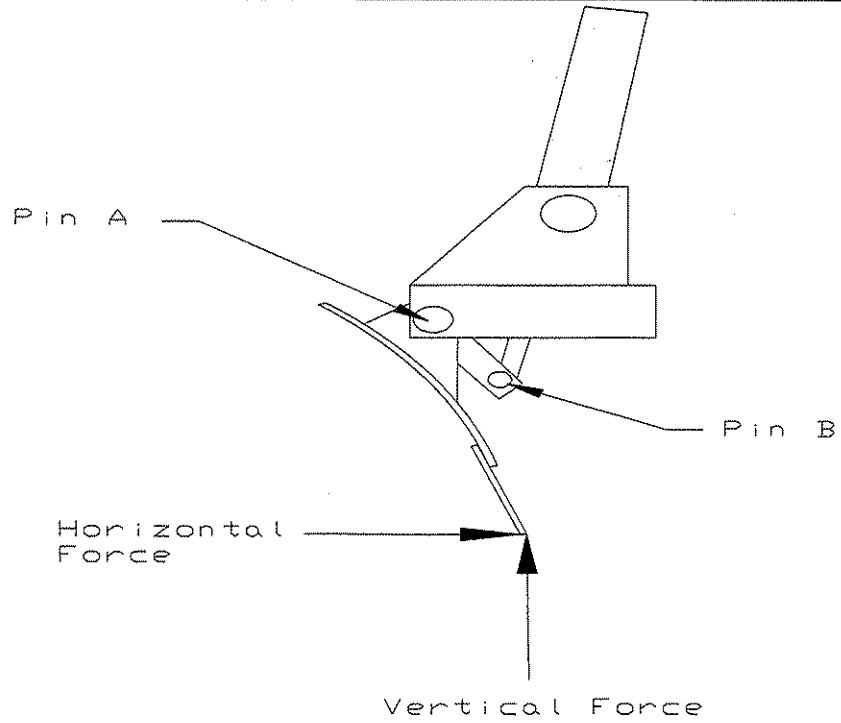


Figure 48 Descriptive placement of Pin A and Pin B relative to the horizontal and vertical force

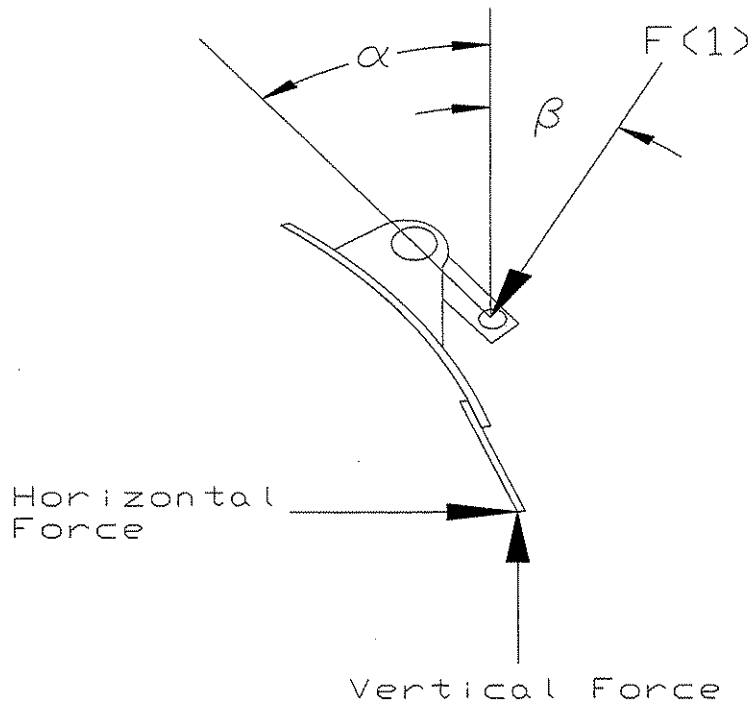


Figure 49 Descriptive placement of α , β and $F(1)$

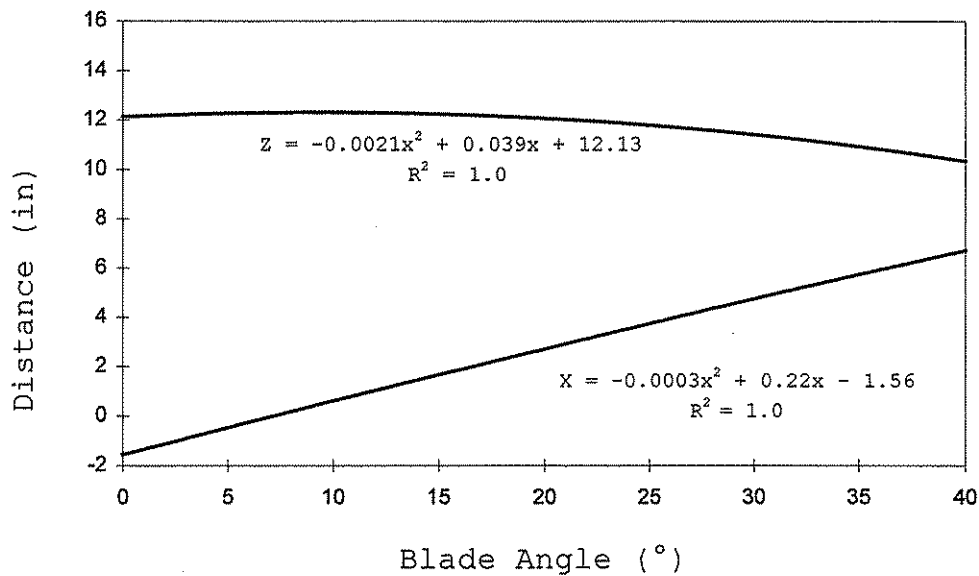


Figure 50 Plot of "X" and "Z" values for a six inch blade

with respect to pin A. Determining the moment about pin A by F(1) is not simply the force multiplied by the distance because the force is not perpendicular to the moment arm. By knowing α and β , the percentage of F(1) that produces a moment about pin A can be determined. Figure 48 shows a close up of pin A, pin B and the force vector representing the 3rd cylinder. Figure 48 shows a new angle, λ (lambda), that is used in calculating the moment produced by F(1).

The moment produced by F(1) about pin A can now be determined by the following formula:

$$\text{moment about pin A by F(1)} = 5.8 * F(1) * \text{Cos}[\lambda] \quad (1)$$

Since the sum of the three angles in Figure 48 is 90° , λ can be determined from the following equation:

$$\lambda = 90 - \alpha - \beta \quad (2)$$

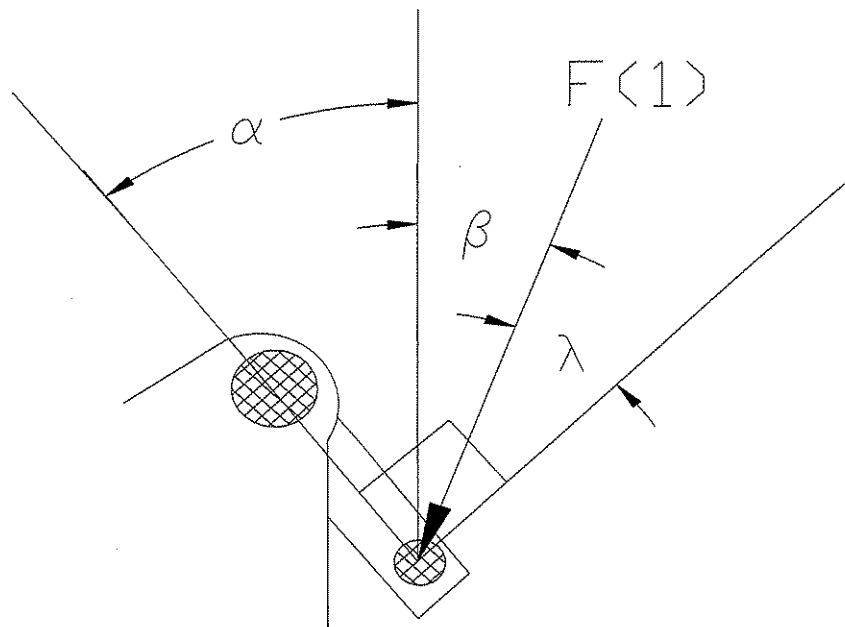


Figure 51 Angles required to determine moment produce by $F(1)$

The angle β can be determined by relating it to the voltage signal produced by the inclinometer. Plotting the angle β verses blade angle shows a linear relationship between the two parameters. This plot is shown in Figure 49.

The angle α can also be determined from the blade angle. By using simple geometry of the underbody, α can be determined from the blade angle from the following equation:

$$\alpha = \text{blade angle} + 15.3^\circ \quad (3)$$

Having expressed α and β in terms of blade angle, λ as well can be solved for in terms of blade angle. The final equation for λ is given as:

$$\lambda = 59.5^\circ - 0.72 * \text{blade angle} \quad (4)$$

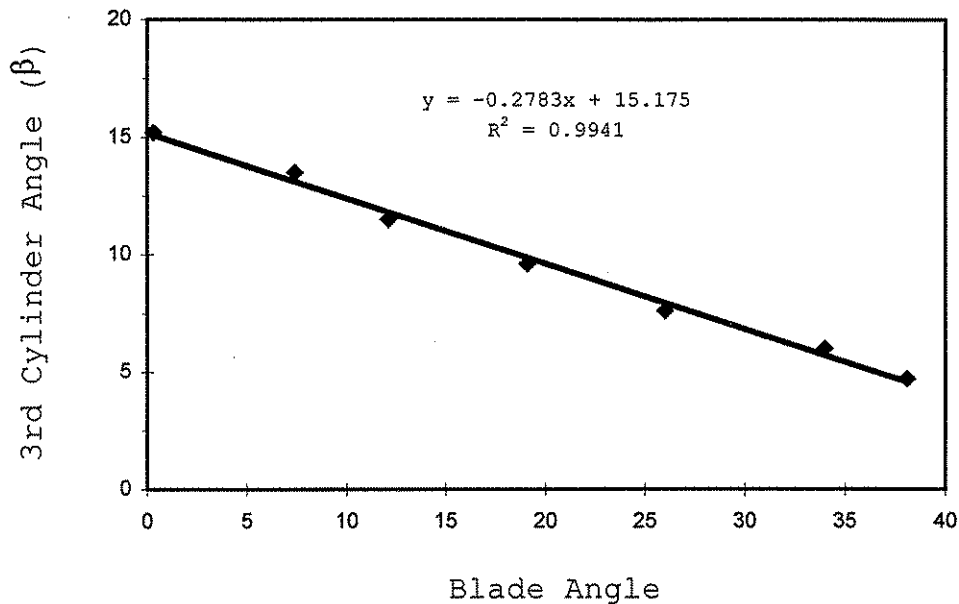


Figure 52 Angle β versus blade angle

The units for λ is in degrees because blade angle expressed above is also in units of degrees.

The final equation for horizontal force is given by summing forces about pin A. Assuming the counter-clockwise direction is positive and that the vertical force will always be located right of pin A, the horizontal force is given as:

$$\text{Horizontal force} = \{ 2 * F(1) * 5.8 * \text{Cos} [59.5 - 0.72 * \text{blade angle}] - \text{Vertical force} * X \} / Z \quad (5)$$

The number "2" in front of F(1) is required because there is two cylinders that are classified as a "3rd cylinder". This equation is only applicable to only snow blades that are six inches in height. Cutting edges that are eight inches in height need to use "X" and "Z" values specifically for an eight inch blade. Figure 50 shows the plot of "X" and "Z" for an eight inch blade.

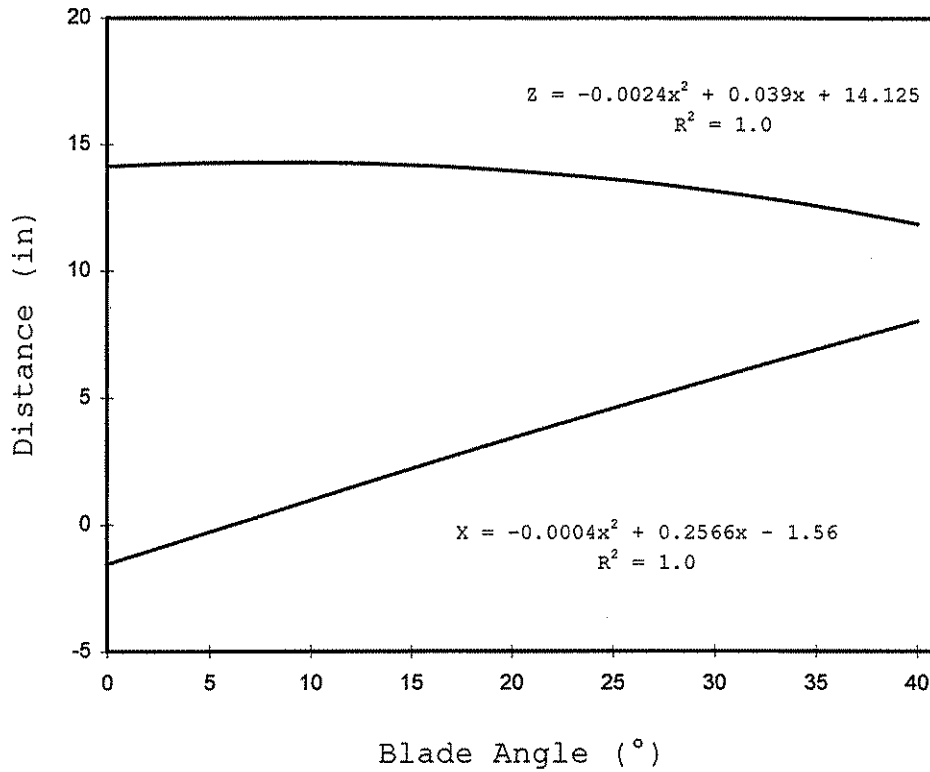


Figure 53 Plot of "X" and "Z" values for an eight inch blade

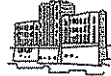


APPENDIX C

In-service results



	Run: 1		Time: 10 min		
	min	max	mean	stdev	
Blade Angle	35	42	38	1	
Vertical Force	6900	13000	7400	600	
Horizontal Force	1900	44400	3200	1400	
Force Angle	16	79	67	3	
	Run: 1		Time: 6 min		
	min	max	mean	stdev	
Blade Angle	36	69	40	4	
Vertical Force	6900	25000	10000	2100	
Horizontal Force	1000	40600	2700	2000	
Force Angle	20	89	72	8	
	Run: 1		Time: 3 min		
	min	max	mean	stdev	
Blade Angle	35	62	38	4	
Vertical Force	7300	14500	8000	600	
Horizontal Force	200	4500	3500	600	
Force Angle	60	89	67	4	
	Run: 1		Time: 6 min		
	min	max	mean	stdev	
Blade Angle	24	69	38	6	
Vertical Force	7200	10700	10200	1800	
Horizontal Force	10	5400	3200	900	
Force Angle	56	89	67	7	
	Run: 1		Time: 3 min		
	min	max	mean	stdev	
Blade Angle	27	64	43	8	
Vertical Force	12000	15000	13100	1100	
Horizontal Force	20	2900	500	400	
Force Angle	78	89	87	2	
	Run: 1		Time: 7 min		
	min	max	mean	stdev	
Blade Angle	21	63	34	9	
Vertical Force	14000	22500	15500	2300	
Horizontal Force	500	3400	1300	700	
Force Angle	57	89	85	3	
	Run: 2		Time: 15 min		
	min	max	mean	stdev	
Blade Angle	0	70	33	20	
Vertical Force	8000	28000	16000	3000	
Horizontal Force	100	9600	4500	2000	
Force Angle	52	89	73	7	



	Run: 2	Time: 21 min			
		min	max	mean	stdev
Blade Angle		-1	69	29	23
Vertical Force		11500	27000	15000	900
Horizontal Force		1500	24000	6300	1900
Force Angle		59	89	67	7
	Run: 2	Time: 7 min			
		min	max	mean	stdev
Blade Angle		-2	65	8	11
Vertical Force		10200	23000	12000	600
Horizontal Force		600	9200	7000	1800
Force Angle		52	89	60	7
	Run: 2	Time: 23 min			
		min	max	mean	stdev
Blade Angle		-3	66	23	22
Vertical Force		9000	26000	21000	2000
Horizontal Force		20	11000	7500	2400
Force Angle		48	89	69	8
	Run: 2	Time: 7 min			
		min	max	mean	stdev
Blade Angle		-3	61	13	14
Vertical Force		21000	31000	22000	600
Horizontal Force		1100	10700	7800	1500
Force Angle		49	89	70	4
	Run: 3	Time: 65 min			
		min	max	mean	stdev
Blade Angle		-4	69	20	25
Vertical Force		6800	27000	20000	3000
Horizontal Force		100	11500	7200	2500
Force Angle		64	89	72	6
	Run: 4	Time: 9 min			
		min	max	mean	stdev
Blade Angle		-2	59	15	13
Vertical Force		7000	17000	8000	800
Horizontal Force		250	8300	5600	1500
Force Angle		45	88	55	8
	Run: 4	Time: 64 min			
		min	max	mean	stdev
Blade Angle		-3	71	38	25
Vertical Force		6000	32000	9600	2000
Horizontal Force		100	19000	4300	2200
Force Angle		21	89	67	10



	Run: 5		Time: 49 min	
	min	max	mean	stdev
Blade Angle	-31	69	27	7
Vertical Force	6000	29000	8500	1800
Horizontal Force	1100	72000	3600	2200
Force Angle	49	89	63	7

	Run: 6		Time: 73 min	
	min	max	mean	stdev
Blade Angle	-3	53	9	10
Vertical Force	7000	25000	10000	1200
Horizontal Force	100	17000	6400	1100
Force Angle	29	89	57	7

	Run: 7		Time: 13 min	
	min	max	mean	stdev
Blade Angle	0	57	26	17
Vertical Force	6800	26000	14000	4000
Horizontal Force	100	13000	3600	2000
Force Angle	29	89	75	6

	Run: 7		Time: 6 min	
	min	max	mean	stdev
Blade Angle	-1	34	10	9
Vertical Force	12000	17000	14000	800
Horizontal Force	200	8800	5800	2400
Force Angle	57	89	68	9

	Run: 7		Time: 53 min	
	min	max	mean	stdev
Blade Angle	-2	56	19	12
Vertical Force	7000	20500	10000	2000
Horizontal Force	100	9150	5100	1500
Force Angle	42	89	60	9